Quaternary International 408 (2016) 93–112

Contents lists available at ScienceDirect

Quaternary International

journal homepage: www.elsevier.com/locate/quaint

Rapid evolution of coastal lagoons in response to human interference under rapid sea level change: A south Caspian Sea case study

Safiyeh Haghani [a, *], Suzanne A.G. Leroy [a], Frank P. Wesselingh [b], Neil L. Rose [c]

[a] Environmental Science, Brunel University London, London, UB8 3PH, UK
[b] Naturalis Biodiversity Centre, Leiden, Netherlands
[c] Environmental Change Research Centre, University College London, London, WC1E 6BT, UK

ARTICLE INFO

Article history:
Available online 11 January 2016

Keywords:
Short-lived coastal lagoons
Rapid Caspian Sea level change
Sediment
Palaeoecology
Conservation

ABSTRACT

This paper examines the interdependence of different factors in the evolution of a coastal lagoon system of the Sefidrud Delta (SW Caspian Sea) based on multi-proxy sedimentary and palaeoecological analyses and remotely sensed data. According to historical aerial photographs and multiple strands of chronology, these coastal lagoons formed between 1955 and 1964, when the sea-level was relatively stable. However, formation of barrier-lagoon systems due to sea level rise is quite typical in different areas of the world, but in this case study high sediment input and longshore currents were the main driving mechanisms that permitted the establishment of a sand spit complex. After 1964, the evolution of these coastal lagoons has been mainly controlled by changing sediment input due to dam construction and rapid sea-level fluctuation. Dam flushing operations and rapid sea-level rise (~3 m between 1977 and 1995) have accelerated the infilling of the coastal lagoon system. This rapid infilling (3.1 cm y^{-1}) makes the whole system more prone to sediment encroachment in the short term. Because the lagoons are short-lived and have a dynamic evolution, rapid natural changes interact with anthropogenic modifications of the Caspian Sea environments. The short-lived nature of these lagoonal systems (total duration of 115 years for Zibakenar Lagoon) can be used as a model for lagoonal development and evolution, in other places in the world. The Caspian coast and the lagoons along it may provide a natural laboratory for what might happen in other lagoons along other coasts in the world, in response to global sea level fluctuation.

© 2015 The Authors. Published by Elsevier Ltd. This is an open access article under the CC BY-NC-ND license (http://creativecommons.org/licenses/by-nc-nd/4.0/).

1. Introduction

The Caspian Sea (CS) with a surface area of 371,000 km^2, comparable in size with the British Isles, has experienced a ~3 m fall and rise during the 20th century (Fig. 1), while the global sea level has fluctuated approximately 2 mm/year in the same period (Kroonenberg et al., 2007). The CS offers a unique opportunity to downscale the long-term impacts of global sea level changes on coastal environments in a short time frame. Although the CS is technically a lake (Fig. 2A), its 'sea-like'—size and nature is reflected in the terminology (sea-level changes). These rapid level changes have impacted global climate (Arpe et al., 2012; Farley-Nichols and Toumi, 2014) and the lives of more than 10 million people around the CS (Dolotov and Kaplin, 2005; Kosarev, 2005; Rucevska et al., 2006; Leroy et al., 2010). Coastal geomorphology has also undergone rapid and varied changes in response to the lake level changes including passive inundation, beach-ridge formation, barrier-lagoon development and general erosion (Kaplin and Selivanov, 1995; Naderi Beni et al., 2013a). On the southern (Iranian) CS coast, major changes occurred in the Sefidrud Delta where the lagoons of Zibakenar, Ushmak and Kiashahr have developed (Fig. 2B) (Kousari, 1986; Lahijani et al., 2009; Leroy et al., 2011; Naderi Beni et al., 2013a). The lagoons are part of the Boujagh National Park, a hotspot for birds (such as cranes and pelicans) and fish (e.g. sturgeons and salmon) (Naqinezhad et al., 2006; Yousefi et al., 2012). This study focuses especially on the Zibakenar Lagoon and its infill in order to investigate the evolution of this short-lived lagoon through the lens of rapid sea-level changes. The aim of this paper is to determine when these coastal lagoons started to form, the main driving forces over time, the rate of changes and the future of this lagoonal system. The study emphasises the effects of short-term natural changes in the coastal lagoons in relation to

* Corresponding author.
E-mail address: safiyeh.haghani@gmail.com (S. Haghani).

http://dx.doi.org/10.1016/j.quaint.2015.12.005
1040-6182/© 2015 The Authors. Published by Elsevier Ltd. This is an open access article under the CC BY-NC-ND license (http://creativecommons.org/licenses/by-nc-nd/4.0/).

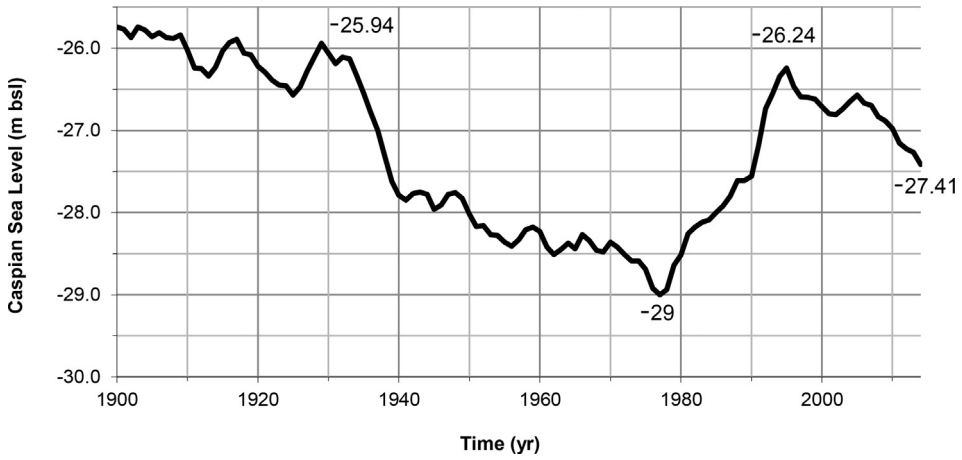

Fig. 1. Caspian Sea level (CSL) from 1900 to 1992 from Lepeshevkov et al. (1981); from 1992 to 2014 from USDA (2015).

anthropogenic effects, and demonstrates that rapid change is not only due to human action, but also due to rapid sea-level change. In this study, firstly we apply sedimentary and palaeoecological analyses to a sediment core in the Zibakenar Lagoon. Secondly, we combined multiple dating approaches including radionuclide dating, radiocarbon dating, indirect biotic dating and evidence from spheroidal carbonaceous fly-ash deposits with remote sensing techniques to understand the initiation and evolution of the Zibakenar Lagoon.

2. Study area

2.1. General geographical location

The CS is the largest closed water body in the world (Fig. 1A). Salinity in the middle and southern basins of the CS is around 13 practical salinity unit (psu), whereas it is nearly fresh in the northern basin, especially near the Volga Delta. Although most of the fresh water (~80%) is provided by the Volga River, the Sefidrud (= White River; and white has a metaphorical meaning of life-giving in Persian) supplies ~40% of the sediment entering the CS (Lahijani et al., 2008). The source of the 820 km long Sefidrud is in the Zagros Mountains in western Iran. The river passes through a narrow passage within the Alburz Mountains to reach its large delta on the southern CS shore (Lahijani et al., 2008). The Sefidrud Delta is wave-dominated during sea-level rise. During episodes of sea-level fall, the delta becomes river-dominated (Naderi Beni et al., 2013b). The Sefidrud has repeatedly changed its course through the area between the Anzali and Amirkola lagoons (Kousari, 1986) (Fig. 2B). The last major avulsion occurred around AD 1600 when the river diverted its course from the east, near Amirkola Lagoon, towards the west near Kiashahr Lagoon, shifting its outlet ~23 km westwards (Lahijani et al., 2009) (Fig. 2B). Sea level rise has been considered the main cause for river avulsion (Törnqvist, 1993; Törnqvist et al., 1996; Aslan and Autin, 1999; Jones and Schumm, 2009; Makaske, 2001; Overeem et al., 2003; Aslan et al., 2005; Hoogendoorn et al., 2005; Naderi Beni et al., 2013b). Avulsion can be caused by a decrease of river gradient as a result of several interacting processes such as subsidence, flood plain aggradation and sea level rise (Jones and Schumm, 2009; Overeem et al., 2003; Heyvaert and Baeteman, 2008). Furthermore, human activities, including channel diversion for irrigation through artificial and natural levee breaks and channel blockages, can also cause river avulsion (Heyvaert and Baeteman, 2008).

2.2. Lagoons' setting

The coastal lagoons of Zibakenar and Ushmak, located on the west side of Sefidrud, are part of a larger lagoon complex called Boujagh Lagoon (Fig. 2B). Hence, each of these lagoons is also known as the Boujagh (Boojagh, Bojagh) Lagoon. Kiashahr Lagoon (also called Farahnaz), located on the east side of Sefidrud, together with Zibakenar and Ushmak Lagoons, are part of the Boujagh National Park (BNP) (Fig. 2B) which was designated a Ramsar site in 1975. A Ramsar site is an internationally important wetland habitat designated under the Convention on Wetlands, held in 1971 in Ramsar, Iran. Most hunting activities have been banned since 1998 and the area is an important refuge for migratory birds (Naqinezhad et al., 2006). Since 2001, the area has also been designated a national park in order to decrease threats to its vegetation cover and to protect its biodiversity (Naqinezhad, 2012). The site is used for recreational and commercial fishing including aquaculture, livestock grazing, reed-cutting, limited hunting, rice farming and recreation/tourism (Annotated Ramsar List, 2011). The depth of water in these lagoons is usually less than 2 m, controlled by the level of the water table, and also by freshwater input through precipitation and irrigation.

2.3. Source of the sediments

Most of the coarse sediments in the study area are transported to the coast by the Sefidrud. Passing through a barren plateau and steep mountains, the Sefidrud, with a mean sediment discharge of ~32 million tonnes per year, provides a huge amount of eroded sediments to the CS shoreline (Lahijani et al., 2008). The south-western rivers including the Sefidrud, Kura, and Terek Rivers supply around 79% of sediment to the CS (42, 22, and 15%, respectively) (Lahijani et al., 2008). These sediments are redistributed mainly by waves and wave-induced longshore currents. The prevailing currents are southward in Azerbaijan and along the west Iranian coast (Lahijani et al., 2009). With the latter currents, sediments originating from the western rivers (e.g. Kura River) also contribute to the sediment supply in the area (Doriniana and Myakokin, 1972). These longshore currents supply sediment for the development of spit-barrier systems and associated lagoons (Kaplin and Selivanov, 1995; Kroonenberg et al., 2000; Lahijani et al., 2009) such as the Anzali, Zibakenar, Kiashahr and Amirkola lagoons (Kousari, 1986; Lahijani et al., 2009; Naderi Beni et al., 2013b). Furthermore, the prevalent winds, combined with proximal availability of barren

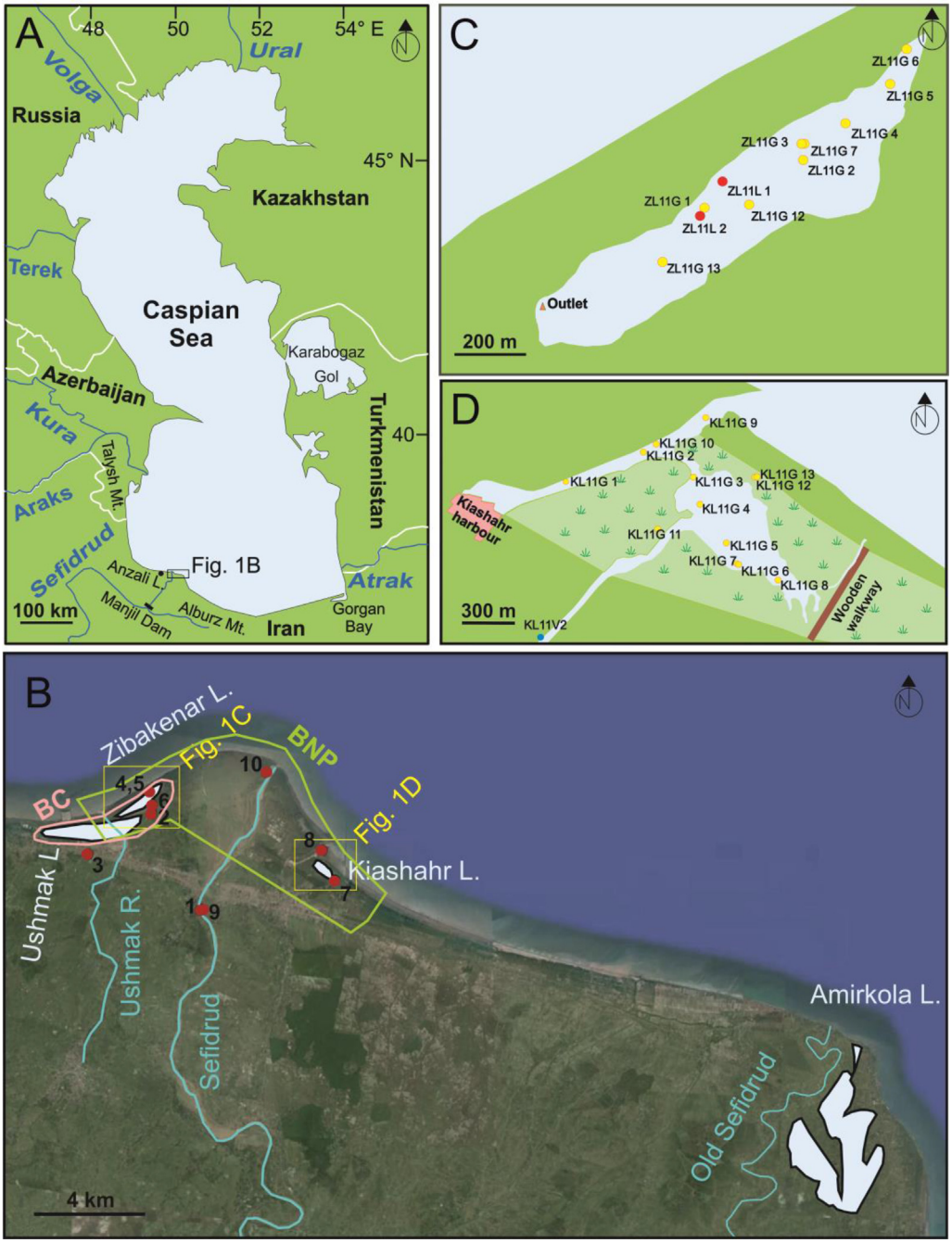

Fig. 2. A: Location map of the Caspian Sea (white lines represent international boundaries.) and major rivers flowing to the Caspian Sea. Mt.: Mountains; B: The location of Zibakenar, Ushmak, Kiashahr and Amirkola Lagoons (Google Earth), green line represents Boujagh National Park (BNP) boundary from Naqinezhad (2012), pink line represents Boujagh complex (BC) including Zibakenar and Ushmak lagoons and red dots represent the location of surface pollen samples (Table 1), L.: Lagoon, R.: river; C: Location of cores taken from Zibakenar Lagoon. The red dots represent the location of core taken by Livingstone corer and the yellow dots the location of cores taken by gravity corer. D: Location of cores taken from Kiashahr Lagoon. The yellow dots indicate the location of cores taken by gravity corer and the blue dot represents the location of a core taken by percussion corer.

sand sources, drive some dune formation in the delta (Kazancı et al., 2004; Lahijani et al., 2009).

The construction of the Manjil Dam (Fig. 2A) on the Sefidrud in 1962 caused a strong reduction of sediment supply to the lower reaches of the river. The dam, which is also known as the Sefidrud Dam, was constructed on the river in the Manjil area with the purpose of irrigating rice paddies during the summer (Morris and Fan, 1998; Khosronejad, 2009). Approximately 48 million tonnes of sediment enter the reservoir per year. Under normal conditions (without flushing) only 14 million tonnes leave the reservoir annually (Morris and Fan, 1998; Khosronejad, 2009). By 1978, 40% of the Manjil Dam reservoir capacity was choked with sediments and winter sediment flushing operations had to be initiated in 1980 (Morris and Fan, 1998; Khosronejad, 2009; Yamani et al., 2013). Sediment removal varies from year to year, with a maximum of 135 million tonnes of sediment removed in the flushing period of 1984–1985 (Table 1; Morris and Fan, 1998; Yamani et al., 2013). Since 1998, flushing operations have been suspended due to climate variations and increasing periods of drought in Iran (Yamani et al., 2013).

Table 1
Flushing operation statistics from 1980 to 1998, Water Research Institute, Ministry of Energy, Iran as in Yamani et al. (2013). Since 1998 the flushing operations have been suspended due to climate variations and increasing periods of drought in Iran (Yamani et al., 2013).

Flushing period	Sediment discharge (10^6 t)		Water discharge (10^6 m^3)	
	Flushing period	Normal condition (the rest of the year)	Flushing period	Normal condition (the rest of the year)
1980–1981	21.30	9.90	536	4926
1981–1982	10.30	3.8	390	3154
1982–1983	48.80	14.8	1513	4365
1983–1984	72.50	12.2	1017	3747
1984–1985	135.30	9.8	1606	4564
1985–1986	43.80	5.90	1084	3019
1986–1987	31.60	5.60	978	2902
1987–1988	59.10	35.30	1812	6577
1988–1989	55.20	4.70	1057	2636
1989–1990	31.9	1.50	681	2827
1990–1991	23.3	3.20	664	2473
1991–1992	18.6	9.30	664	4796
1992–1993	22.2	6.90	605	3996
1993–1994	52.9	5	2321	5447
1994–1995	46.1	7.70	2136	4489
1995–1996	12.5	10.30	812	4703
1996–1997	15.9	2.10	867	1815
1997–1998	11	3.40	374	3823

The grey shade represents maximum sediment discharge.

3. Materials and methods

3.1. Remote sensing

In the CS area, the recent evolution of the Sefidrud Delta has been documented by comparison of historical aerial photographs. The original work was made by Kousari (1986) and was later supplemented by other publications (i.e. Krasnozhon et al., 1999; Khoshraftar, 2005; Lahijani et al., 2008; Kazancı and Gulbabazadeh, 2013). Based on an updated compilation, our study especially focuses on the evolution of coastal lagoons using aerial photographs of the year 1955, 1964, and 1982, and 1991 and 2014 satellite images from Google Earth. This comparison allowed us to reconstruct not only sand spit formation and development of coastal lagoons, but also minor river avulsions and variations in the morphological features of the delta during the past 59 years.

3.2. Sediment coring

Sediment cores with a maximum composite depth of 220 cm were taken using a gravity corer, a percussion corer and a Livingstone corer during the field campaign organised by the Iranian National Institute for Oceanography and Atmospheric Science (INIOAS) in 2011 from Zibakenar (Fig. 2C) and Kiashahr Lagoons (Fig. 2D). Coring was made from a platform, as water depth around the middle of Zibakenar Lagoon (e.g. ZL11L1 and ZL11L2) is 185 cm. In the Kiashahr Lagoon, water depth reaches 120 cm (e.g. KL11G5). In some locations, duplicate cores were obtained, using the Livingstone corer (i.e. ZL11L2 A and B; ZL11L1 A, B, C and D), and in one situation up to four cores (ZL11L1 A, B, C and D) were taken from the same location. These parallel cores were used to cover gaps between the core sections, to obtain a continuous master sequence.

3.3. Sedimentology

Magnetic susceptibility (MS) measurements were performed on all the cores using a Bartington MS2C core logging sensor at 2 cm intervals. A standard visual core description was performed immediately after core photography (Mazzullo et al., 1988). Sediment colour was determined using a Munsell Colour Chart. Grain size and LOI analyses were performed on the longest sequence from the Zibakenar Lagoon (core ZL11L2). The grain size was determined on 67 samples using a CILAS 1180 particle size analyser on homogenised subsamples and representative facies. Soaking the samples in 10% tetra-sodium pyrophosphate solution and 20 s of ultrasound were used to prevent flocculation. Granulometric data were processed using the GRADISTAT program (Blott and Pye, 2001). The sand-silt–clay triangular diagram proposed by Folk (1974) was used for naming the textural group of the sediments. In addition, the particle size results have been presented in a 3D plot using MATLAB software version 7.1 to highlight detailed changes over depth. Organic matter (OM) and calcium carbonate ($CaCO_3$) were determined through loss on ignition (LOI) (Heiri et al., 2001). All these analyses were performed in the sediment laboratory, Environmental Science, Brunel University London.

3.4. Macro-remains

Following the method of Birks (2001), thirteen samples with a weight of 15–20 g from the master sequence ZL11L2A were deflocculated using 10% tetra-sodium pyrophosphate solution. The samples were then washed through a column of sieves with mesh diameters of 500, 125 and 53 μm. The finest fraction (53 μm) was used to retrieve microfossils such as foraminifers (Leroy et al., 2013). The residue from each sieve was studied using a stereomicroscope (magnifications up to ×90). The samples above 500 and 125 μm were counted; however the finest fraction was only scanned. The results are presented in percentage and concentration diagrams using the Psimpoll software, version 4.27 (Bennett, 2007). A zonation by CONISS after square-root transformation of the percentages and concentration data was applied. Minerals found in the macro-remains at the bottom of ZL11L2A master sequence were identified by X-ray diffraction (XRD) at the Experimental Techniques Centre (ETC), Brunel University London, using a Bruker D8 Advance equipped with a Lynx-eye position–sensitive detector.

3.5. Palynology

Sixteen core samples from the ZL11L2A-B master sequence with a volume of 0.5–1.5 ml were taken for analyses. Most samples came from core A, with only one from core B, at 86.5 cm depth. In addition, ten surface samples (moss pollsters and mud) were

analysed (Fig. 2B; Table 2) in order to provide an idea of the representation of the present-day vegetation in the pollen assemblages and the suitability of various facies.

Table 2
Description of the surface pollen samples.

Sample ID	Site name	Type of sample	Latitude N Longitude E	Sampling date	Description of location
1	Sefidrud bridge	moss	37 25 05.6 49 54 42.8	06/05/2005	on tree, western Sefidrud delta, bridge over main distributary
2	Zibakenar wall	moss	37 27 01.4 49 53 22.5	27/06/2008	at main observation tower on house wall
3	Zibakenar garden	moss	37 26 09.1 49 51 46.8	27/06/2008	garden of restaurant at tree foot
4	Zibakenar hand	mud	37 27 27.7 49 53 17.6	27/06/2008	in *Phragmites* belt, by hand
5	Zibakenar HCGA11	mud	37 27 27.7 49 53 17.6	27/06/2008	in open lake very near to edge, grab
6	Zibakenar st shore	mud	37 27 11.9 49 53 23.0	30/10/2011	sandy mud, at point of boat loading for the station, recently submerged by rise in lake level, path between emerged vegetation belt
7	Kiashahr grab	mud	37 25 47.9 49 58 07.2	27/06/2008	from wooden bridge in a wide *Phragmites* area, very polluted, brown water, oil film
8	Kiashahr KG10	mud	37 26 23.9 49 57 46.5	28/10/2011	black mud, in channel to CS, Juncus/Cyperaceae, along artificial stone wall
9	Sefidrud SS1	mud	37 25 06.5 49 54 44.8	30/10/2011	fine sediment along Sefidrud: sterile
10	Sefidrud tip	mud	37 27 56.4 49 56 17.5	18/05/2011	rive side mud, a few tens of m from tip of delta, clayey layer at base of plants: sterile

The sediment samples were soaked in 10% tetra-sodium pyrophosphate solution for deflocculation. The samples were then treated with cold HCl (first at 10% and then pure), cold HF (32%), followed by a repeated cold HCl treatment, in order to eliminate carbonates, quartz and fluorosilicate gels, respectively. Finally, the samples were sieved through 125 and 10 μm nylon meshes. The mosses were additionally acetolysed. The residues were mounted on glass slides in glycerol. The initial addition of *Lycopodium* tablets allowed the estimation of concentrations (number of palynomorphs per ml of wet sediment).

Dinocysts were identified using the studies of Marret et al. (2004), Leroy et al. (2006) and Leroy (2010). Percentages of pollen, non-pollen palynomorphs and dinocysts were calculated on the sum of land-derived pollen (or terrestrial) only, with a median of 308 terrestrial pollen grains for the core samples and 322 for the surface samples. A zonation by cluster analysis (CONISS) after square-root transformation of the percentage data was applied to the main terrestrial taxa of the core samples.

3.6. Chronology

A variety of direct and indirect tools has been used for dating of the ZL11L2 sequence. Radionuclide analyses were made on the first core section (i.e. ZL11L2A1) and also on three additional samples on the second section (i.e. ZL11L2A2) at University College London. The implemented radionuclides include ^{210}Pb (half-life = 22.3 year), a naturally-produced radionuclide derived from atmospheric fallout (termed unsupported ^{210}Pb), ^{137}Cs (half-life = 30 years) and ^{241}Am, artificially produced radionuclides introduced to the study area by atmospheric fallout from 1950s nuclear weapons testing. Dried sediment samples were analysed for ^{210}Pb, ^{226}Ra, ^{137}Cs and ^{241}Am by direct gamma assay using ORTEC HPGe GWL series well-type coaxial low background intrinsic germanium detectors. ^{210}Pb was determined via its gamma emissions at 46.5 keV, and ^{226}Ra by the 295 keV and 352 keV gamma rays emitted by its daughter isotope ^{214}Pb following three weeks storage in sealed containers to allow radioactive equilibration. ^{137}Cs and ^{241}Am were measured by their emissions at 662 keV and 59.5 keV (Appleby et al., 1986). The absolute efficiencies of the detector were determined using calibrated sources and sediment samples of known activity. Corrections were made for the effect of self-absorption of low energy gamma rays within the sample (Appleby et al., 1992).

Three radiocarbon dates were obtained on plant remains at the Chrono Centre, Queen's University of Belfast, UK. Radiocarbon ages younger than AD 1950 (modern ages) were calibrated using the CALIBomb programme (Reimer et al., 2004) with the Northern Hemisphere zone 2 calibration dataset (Hua et al., 2013). The date older than AD 1950 was calibrated using the CALIB programme version 7.1 (Stuiver and Reimer, 1993) with the IntCal13 calibration curve (Reimer et al., 2013).

As part of the indirect dating tools, identification of spheroidal carbonaceous fly-ash particles (SCPs), unambiguous indicators of industrial fossil-fuel combustion, was performed at University College London to identify recent sediments. A rapid increase in SCP accumulation rate at 1950 ± 5 years was also used to compare with the radiometric chronology (Renberg and Wik, 1984, 1985; Rose et al., 1995, 2003). SCP extraction from sediments followed the method of Rose (1994), while SCP identification used standard criteria (Rose, 2008). The occurrence of plant and bivalve species recently introduced by people was also used as indirect dating tools.

4. Results

4.1. Remote sensing

The earliest detailed outline and architecture of the Sefidrud Delta was extracted from the aerial photograph of the year 1955 (Fig. 3A). Kousari (1986) made the first classification that we largely follow here. However, an abandoned channel to the west of Sefidrud was considered as a sand spit by Kousari (1986). Moreover, we were unable to confirm the interpretation of a new sand barrier recognised by Kousari (1986) in front of the Ushmak River. Fig. 3B and C show the evolution of the delta in the years 1964 and 1982. We modified some of Kousari's (1986) interpretations as follows. A feature in the Ushmak Lagoon was recognised by Kousari (1986) from aerial photographs of 1964 and 1982, and was classified as a sand barrier. However, based on the shape of this feature, the presence of sand spits on its two sides and present-day satellite

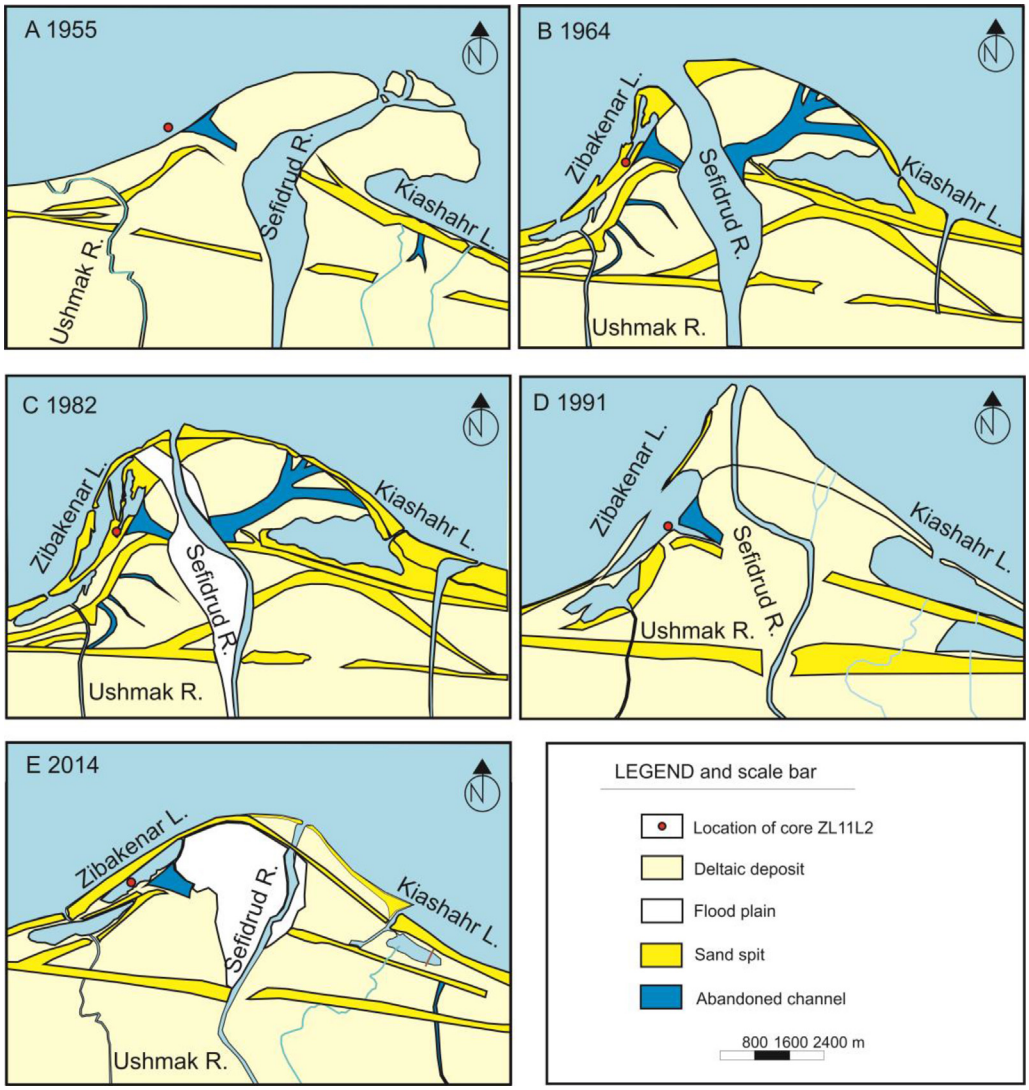

Fig. 3. Evolution of the new Sefidrud Delta since 1955, based on historical aerial photographs (A, B and C) and satellite images (D and E). Fig. 2 B and C after Kousari (1986) with modifications.

photos, we consider it likely that this feature is a coastal lagoon at this time. Moreover, this coastal lagoon is clearly recognisable at this site in the satellite image from the years 1991 and 2014 (Fig. 3D and E). In Kazancı and Gulbabazadeh (2013), neither Zibakenar nor Ushmak Lagoons were plotted for the year 1964, and Zibakenar Lagoon does not appear on the map until 1982. Contrary to the situation for the Zibakenar Lagoon, all studies agree that the Kiashahr Lagoon started to form in 1955.

4.2. Sedimentology

Magnetic susceptibility (MS) results show considerable variation within and among the cores (Figs. 4 and 5). In the Zibakenar Lagoon, the bottom of the long sequences (i.e. ZL11L2A, ZL11L1A and ZL11L1C) yields high MS values, up to 32. In overlying intervals a sharp decrease to values below four is found. Such MS values are also typical for all of the short cores (Fig. 4). In the Kiashahr Lagoon, the cores KL11V2, KL11G12 and KL11G13 in the overgrown lagoon (swamp) contain high MS values (≥20, Fig. 5). The MS values of the cores located in the margin of open water of the lagoon (KL11G3, KL11G6, KL11G7 and KL11G8) and channel (KL11G1, KL11G2, KL11G9 and KL11G10) (see Fig. 2D for locations) show medium MS values, up to five. The MS of the cores located in the open water of the lagoon have the lowest values (~1, Fig. 5).

The Zibakenar Lagoon infill consists of varied sediment layers (Fig. 6). At the base of three long cores (ZL11L2A, ZL11L1A and ZL11L1C), dark grey silty sand is found, overlaid by dark grey silty sand with plant remains. This interval is in turn overlain by olive grey to olive silt with bivalve shells and rootlets. Subsequently, a thin red silt layer is overlain by a thick layer of reddish-brown to yellowish-brown homogenous silt. The top horizon consists of bioturbated reddish-brown to yellowish-brown silt with horizons of dark greyish sandy silt and an organic rich layer (Fig. 6). In relatively shallower places (e.g. Zl11G1, G3, G4 and G6), a layer of very dark greyish silt occurs with abundant remains of emerged aquatic plants.

More specifically, the master sequence ZL11L2 is divided into four sedimentological zones (Sz) (Fig. 7). The granulometric data (Fig. 8) integrated below indicate that all samples are polymodal.

Sz1, 220–182 cm: alternation of dark grey silty sand with plant remains. The upper boundary of this facies is sharp.

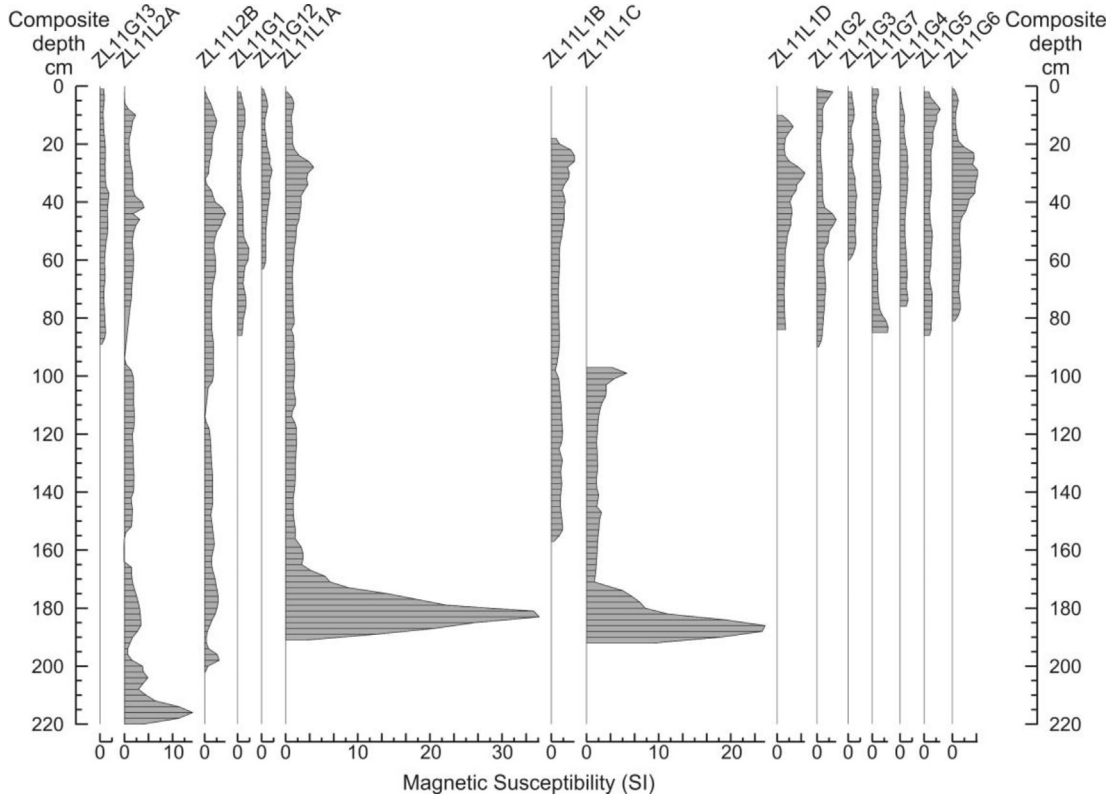

Fig. 4. MS values of the cores taken from the Zibakenar Lagoon. The diagrams are arranged from west (right) to east (left) of lagoon.

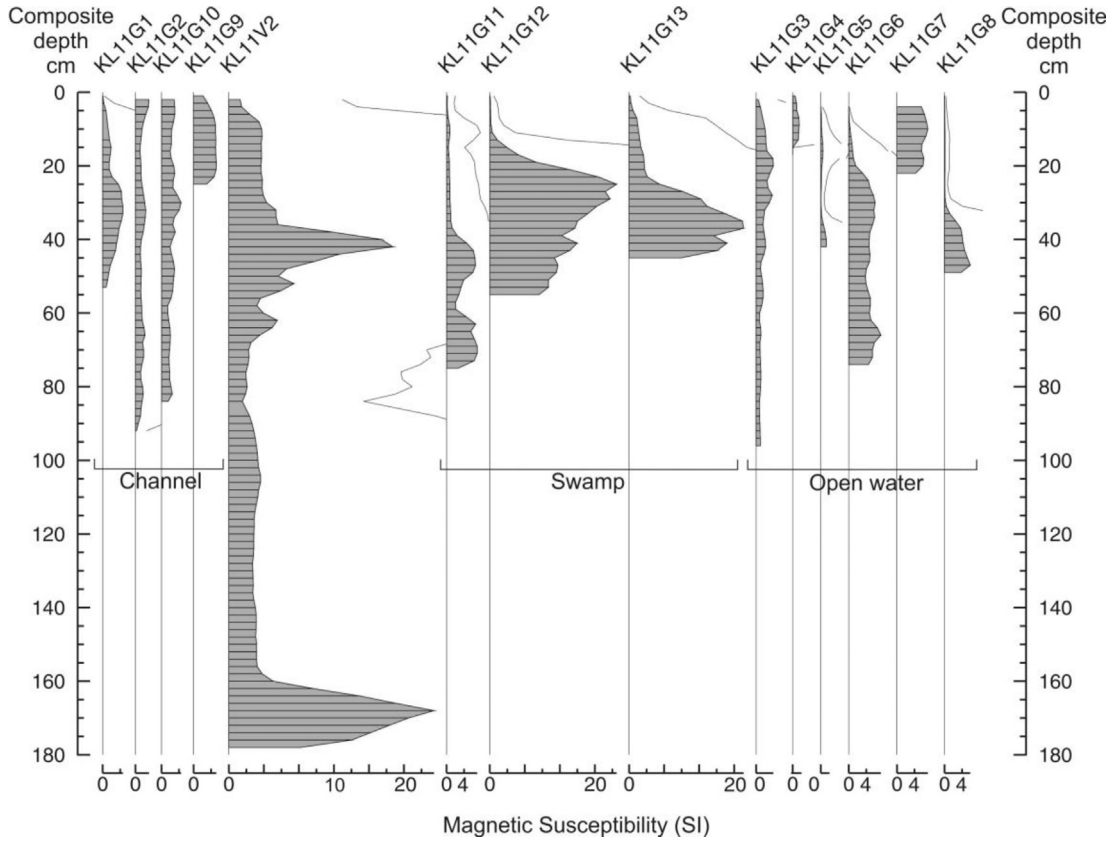

Fig. 5. MS values of the cores taken from the Kiashar Lagoon.

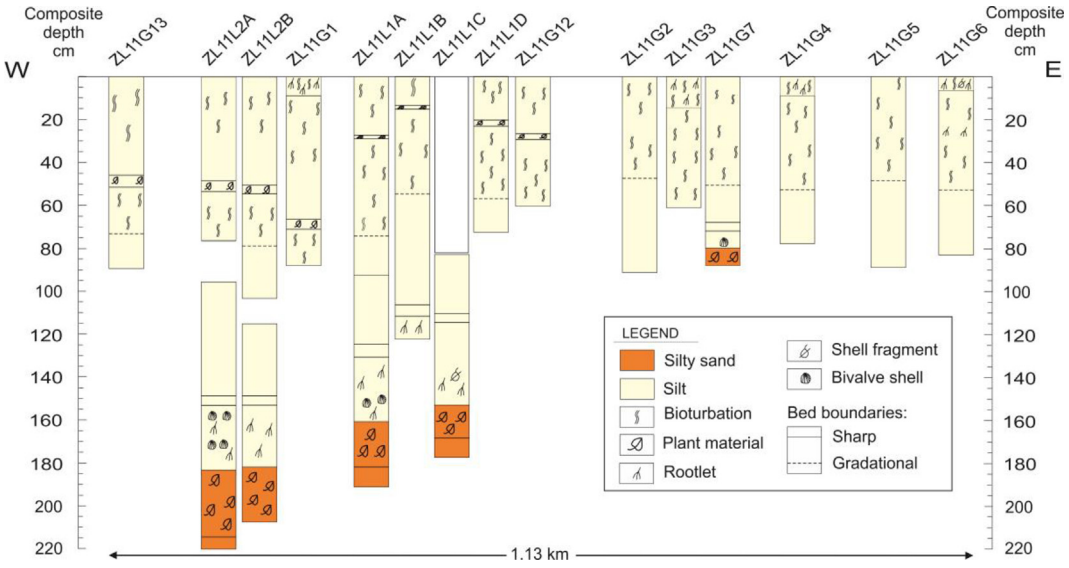

Fig. 6. Sedimentological logs of the cores from the Zibakenar Lagoon. The logs are arranged from the west (left) to the east (right) of the lagoon.

Sz2, 182–147 cm: olive grey silt with a very well preserved bivalve pairs of *Cerastoderma glaucum* at 171 cm and *Dreissena polymorpha* at 160 cm depth. This facies is delimited sharply by the overlying red silt layer (151–147 cm) that appears a significant correlative horizon.

Sz3, 147–76 cm: reddish brown silt with a gradational boundary with the following facies.

Sz4, 76–0 cm: bioturbated reddish–brown silt dark with rootlets and plant material.

The magnetic susceptibility of the master sequence ZL11L2 shows a significant variation along the core (Fig. 7). The results indicate a substantial increase at the base of the core with a peak at a depth of 216 cm. Following this, the MS decreases and is relatively constant along the top 160 cm with two minor peaks at depths of 42 and 10 cm. Overall, the content of organic matter shows a slight ascending trend from the base (Fig. 7). However, the basal 38 cm have two significant peaks of organic matter content at 209 and 197 cm depth with the amounts of 22 and 21%, respectively. The

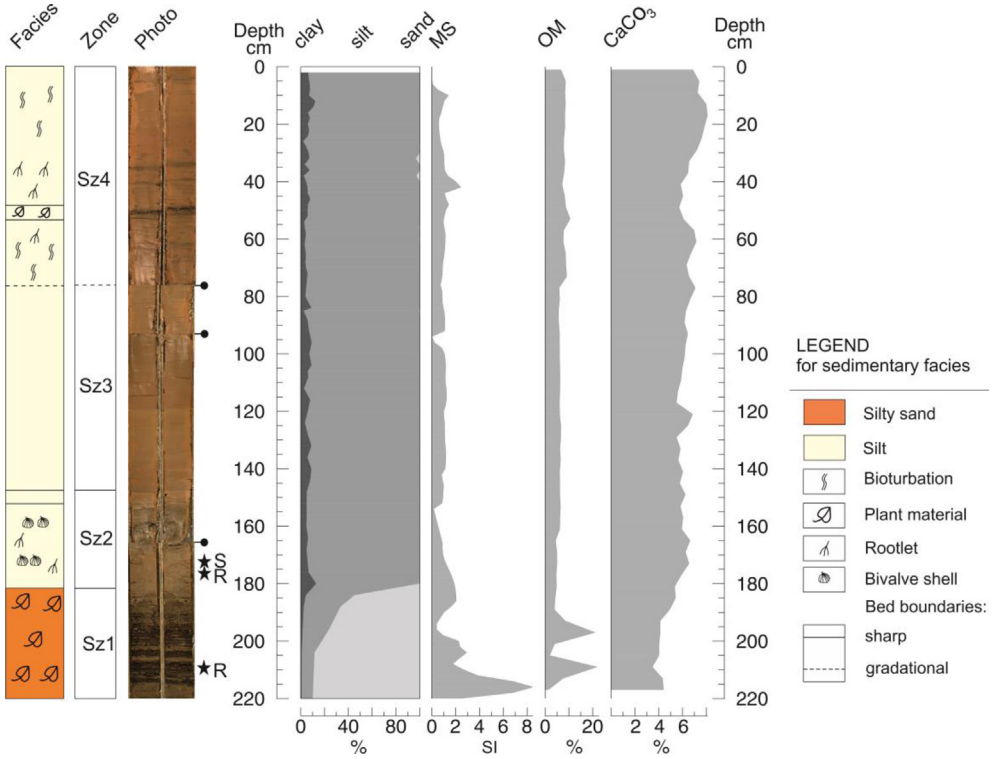

Fig. 7. Sedimentary log for the master sequence (ZL11L2), displaying sedimentology (Sz: sedimentological zone), core photo, grain size (clay, silt and sand), magnetic susceptibility (MS), organic matter (OM) and calcium carbonate (CaCO3). The black stars refer to the depth of the radiocarbon dated samples (R: rootlet, S: shell), and the black pin symbols show the core section limits.

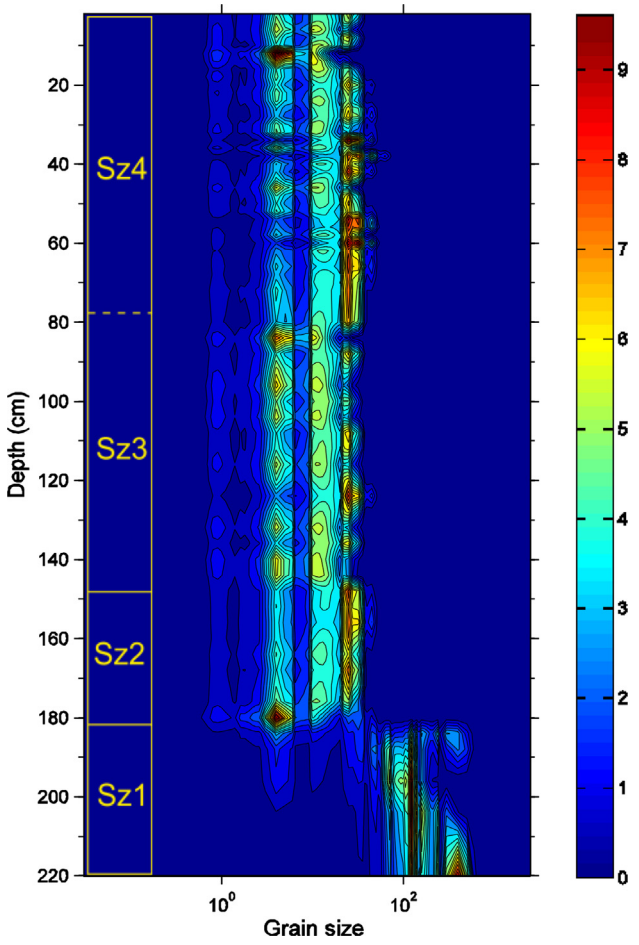

Fig. 8. 3D plot of grain size data (in μm) for the master sequence ZL11L2: the dark blue colour represents the lowest volume (%), while the red colour shows the highest volume (%). Sz: sedimentological zone.

carbonate contents have a background of 4% and vary along the core with a gradual upward increase (Fig. 7).

The Kiashahr Lagoon infill consists of varied sediment layers (Fig. 9). In the open water cores, these layers contain brown silty sand with bivalve shells and rootlets, overlaid by greenish grey and reddish brown silt layers. The silt layer contains rootlets, bioturbation, bivalve and gastropod shells. More silt accumulation is observed in the north-west of the lagoon (e.g. KL11G3 and KL11G4), whereas more silty sand accumulation occurred in the south-east (e.g. KL11G5, KL11G6, KL11G7 and KL11G8).

The cores taken from swampy areas contain brown silty sand with rootlets, plant materials and gastropod shells. Furthermore, a bioturbated layer of reddish brown silt is observed between depths of 40 and 9 cm in core KL11G11. The channel cores mainly contain bioturbated brown silt with rootlets and bivalve shells and thin layers of brown silty sand with bivalve shells and rootlets. Lack of sand in the channel is due to dredging operations associated with an attempt of changing in its economical use from fishing to a commercial port in 2010 (Ramsar Report 37, 2015). Core KL11G9 near the mouth of the channel contains homogenous brown silty sand brought by the CS (Fig. 9). The silty cores of the open lagoon have similarity with the silty cores in the channel, such as silt without bioturbation, overlaid by silt with bioturbation. However, the silty layers in the channel are more brownish and the silty cores of open water contain greyish and brownish layers. It is also likely that the open water cores KL11G3 and KL11G4 consist of true lagoonal sediment whereas the silty cores of the channel may represent recent muds suspended after dredging.

4.3. Macro-remains

In order to simplify the explanation, changes in macro-remains have been described based on the percentages of macro-remains in the 500 μm fraction (Fig. 10and Fig. A1, Appendix A). The main changes for the 125 μm fraction (Fig. 11 and Fig. A2, Appendix A) are added to the descriptions below. Overall, the concentrations of

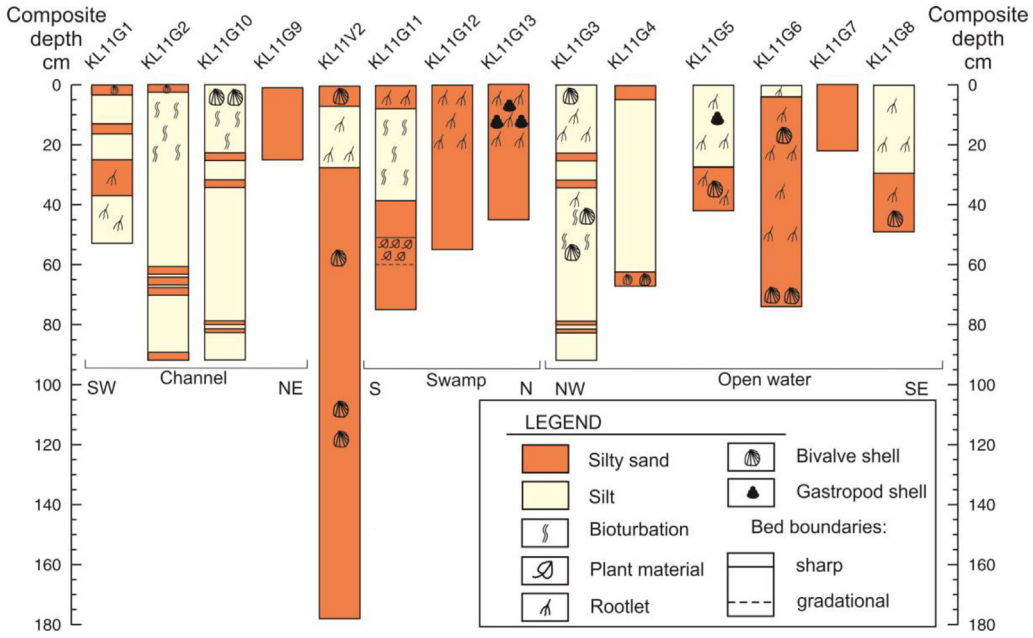

Fig. 9. Sedimentological logs of the cores from the Kiashahr Lagoon.

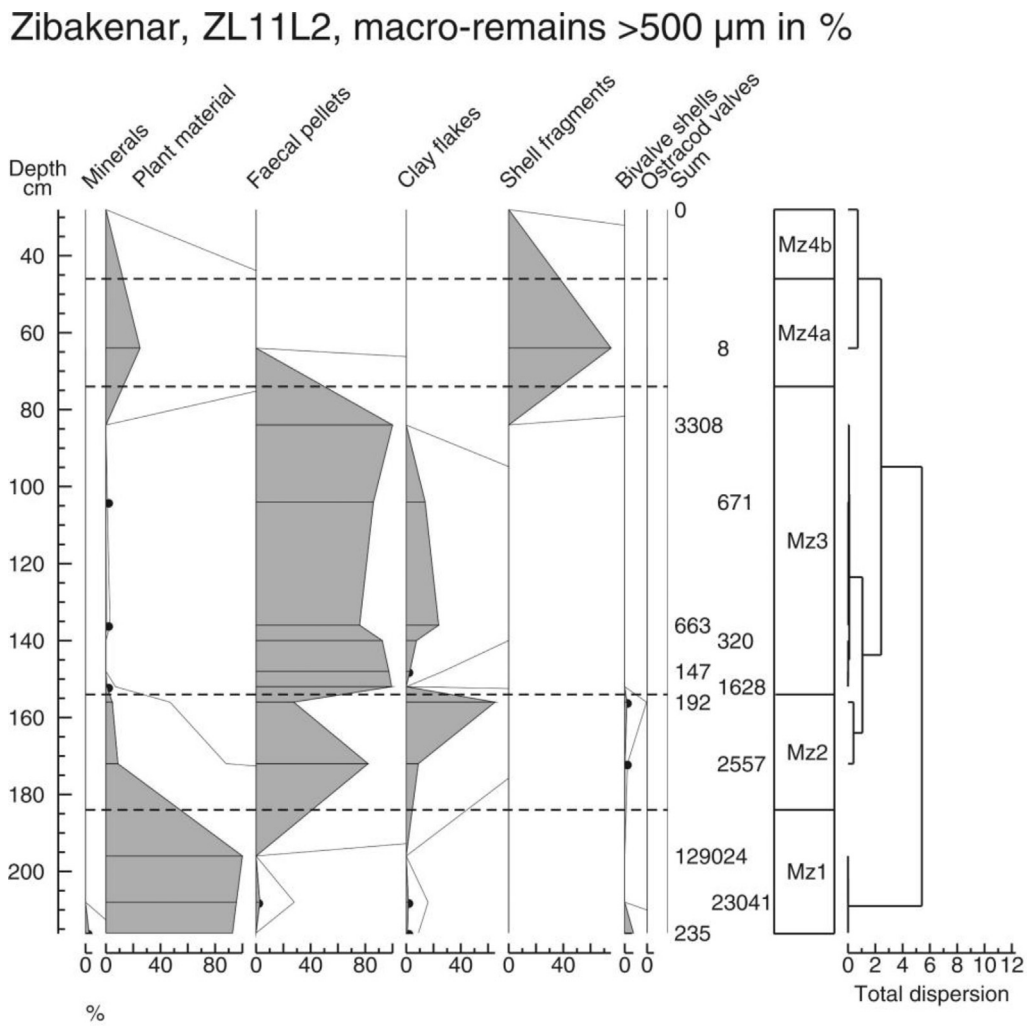

Fig. 10. The percentages of macro-remains above 500 µm in the master sequence ZL11L2. The black dots represent very low percentages of macro-remains.

macro-remains were very high at the base of the sequence and decreased to almost zero at the top. Based on the results, the sequence is divided into four zones.

Mz1, from base to 184 cm (3 samples)

This zone is characterized by maximum abundances of plant material (up to 100%), with some bivalve shells (6.5%), minerals including quartz, plagioclase feldspar, calcite and muscovite (2.5%), faecal pellets (3%) and clay flakes (1.5%). In the fraction of 125 µm, the amounts of mineral and bivalve reach to up to 60% and 14%, respectively. Foraminifer tests (5%) and ostracod valves (9%) appear in the fraction 125 µm. All the observed foraminifers in Zibakenar Lagoon belong to *Ammonia beccarii*. Only larval shells of bivalves are found that either belong to *Monodacna edentula* or to *Cerastoderma glaucum*. *Abra* cf. *segmentum* (earlier this species was reported as *A. ovata*) is found in this zone.

Mz2, from 184 to 154 cm (2 samples)

This zone is characterised by bivalve shells (*A. segmentum* and *M. edentula*/*C. glaucum*) (1.5%), a sharp rise in the amount of faecal pellets (82%) and clay flakes (65%), and a drop in plant materials (9%). Furthermore, 10% minerals, 1% foraminifer tests *(A. beccarii)* and 1% ostracod valves are observed in fraction of 125 µm. Adult bivalve shells including Dreissenidae and *C. glaucum* are observed in this zone.

Mz3, from 154 to 75 cm (6 samples)

The third zone is marked by high values of faecal pellets, especially at a depth of 85 cm, where it even reaches 100%. Moreover, this zone contains clay flakes (0–24%) and only a small amount of plant materials (0.1–1%). In the fraction of 125 µm, this zone is characterised by up to 99% faecal pellets and 23% minerals.

Mz4 a and b, from 75 cm to the surface (2 samples)

This zone is characterized by 25% plant materials and 75% shell fragments and is very poor at 66–64 cm and even barren at 30–28 cm (Fig. A1, Appendix A). However, in the fraction 125 µm, 97% plant material and 3% mineral are identified at a depth of 30–28 cm. Furthermore, 15% foraminifers, 61% faecal pellets and 18% minerals are identified at 66–64 cm.

4.4. Palynology

4.4.1. Recent pollen assemblages

The three moss polsters are characterised by many cultivated and/or introduced plants: *Pinus*, *Eucalyptus*, *Juglans*, *Platanus*,

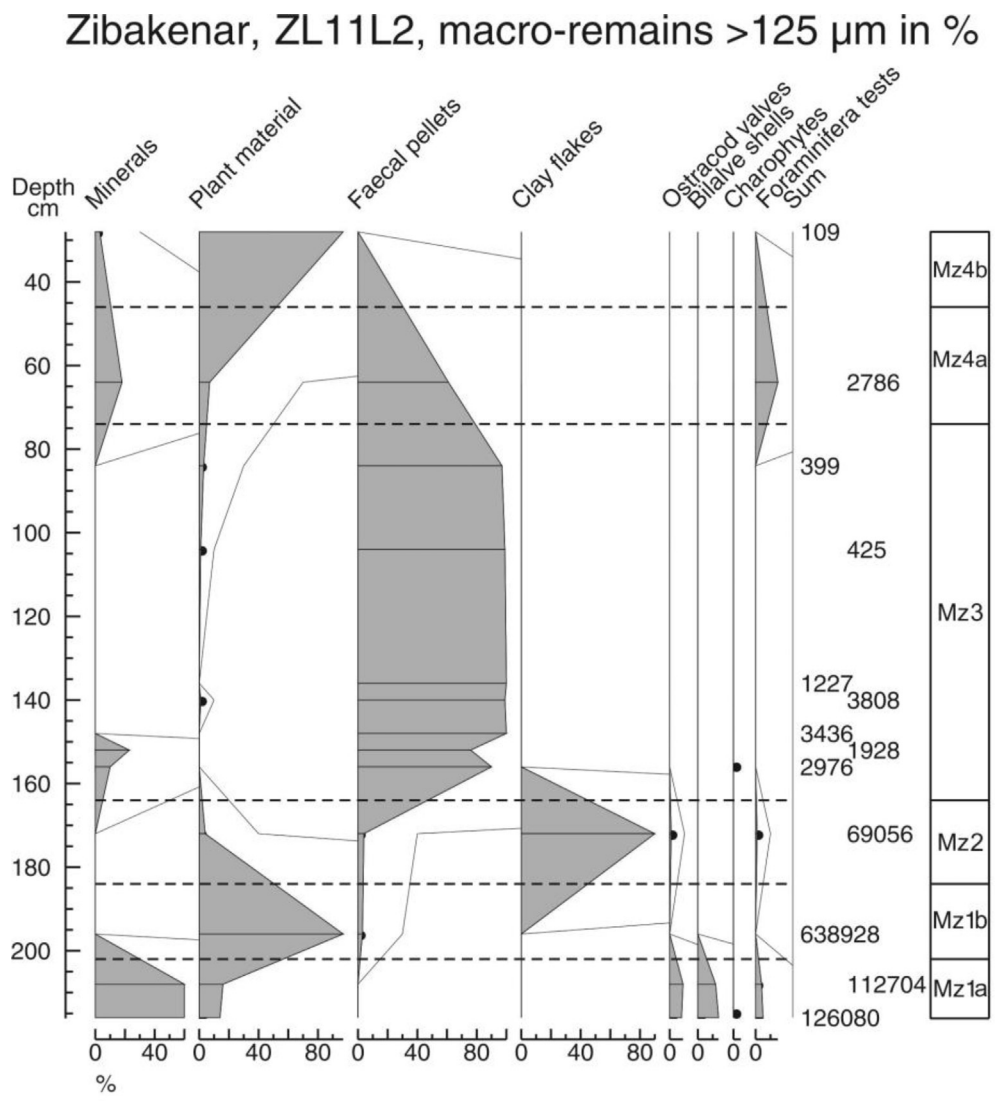

Fig. 11. The percentages of macro-remains above 125 µm in the master sequence ZL11L2. The black dots represent very low percentages of macro-remains.

Cerealia t. and Urticaceae–Moraceae (including the mulberry) (Fig. 12). The *Alnus* values are relatively high (14–31%). Amongst the non-arboreal pollen (NAP), the highest values of *Artemisia* are found (up to 15%). Poaceae are also well represented (12–26%).

The three mud samples from Zibakenar are characterised by relatively low values for *Alnus* (2–13%) and the highest values of Cyperaceae (up to 22%), with some Amaranthaceae, *Artemisia* and Poaceae. In the aquatic percentages, the *Myriophyllum*, *Potamogeton* and *Typha-Sparganium* are relatively abundant. Some samples are extremely rich in fungal spores (483% of the terrestrial pollen sum), including *Glomus*, as well as rich in the Cyanobacteria *Gloeotrichia*. Some rare dinocysts (<2%) but more frequent foraminifers (up to 7%) are present (Fig. 12).

The two Kiashahr muds are characterised by the highest arboreal pollen percentages (46 and 64%) of all surface samples: up to 52% of *Alnus*, 6% of *Carpinus betulus*–t., 2% of *Fagus* and >2% of deciduous *Quercus*. Massulae of the floating fern *Salvinia–Azolla* are observed. The thecamoebians are extremely abundant in one of the samples (up to 357%). Some dinocysts (<4%) and foraminifers (up to 5%) are present (Fig. 12). Two samples from the Sefidrud itself turned out to be barren (Table 2).

4.4.2. Pollen assemblages in the core

The preservation of palynomorphs in the core sequence is generally good, with rare exceptions (e.g. at 134 cm depth) (Fig. 13). The concentrations are low, with usually around 5000 grains/ml, with the exception of the richer top sample (11,500 grains/ml). Three samples are barren between 114 and 94 cm.

The arboreal pollen (AP) is dominated by *Alnus*, with the presence of many other tree pollens such as *Carpinus betulus*, *Fagus*, *Quercus* and *Salix*. The NAP is dominated by Amaranthaceae with frequent Asteraceae, Poaceae and Cyperaceae. The occurrence of Cerealia-t is continuous whilst aquatic pollen and spores are infrequent. The aquatic algae and dinocysts are frequent, but with a noticeable gap in the middle of the sequence. The non-pollen palynomorphs (NPP) are dominated by fungal spores that often have extremely high values. Three pollen zones are defined by well-marked limits:

Pz1, from base to 189 cm

The AP are largely dominated by *Alnus* (up to 62%), with some *Carpinus betulus*, *Fagus*, *Quercus*, *Pterocarya*, *Ulmus–Zelkova* and

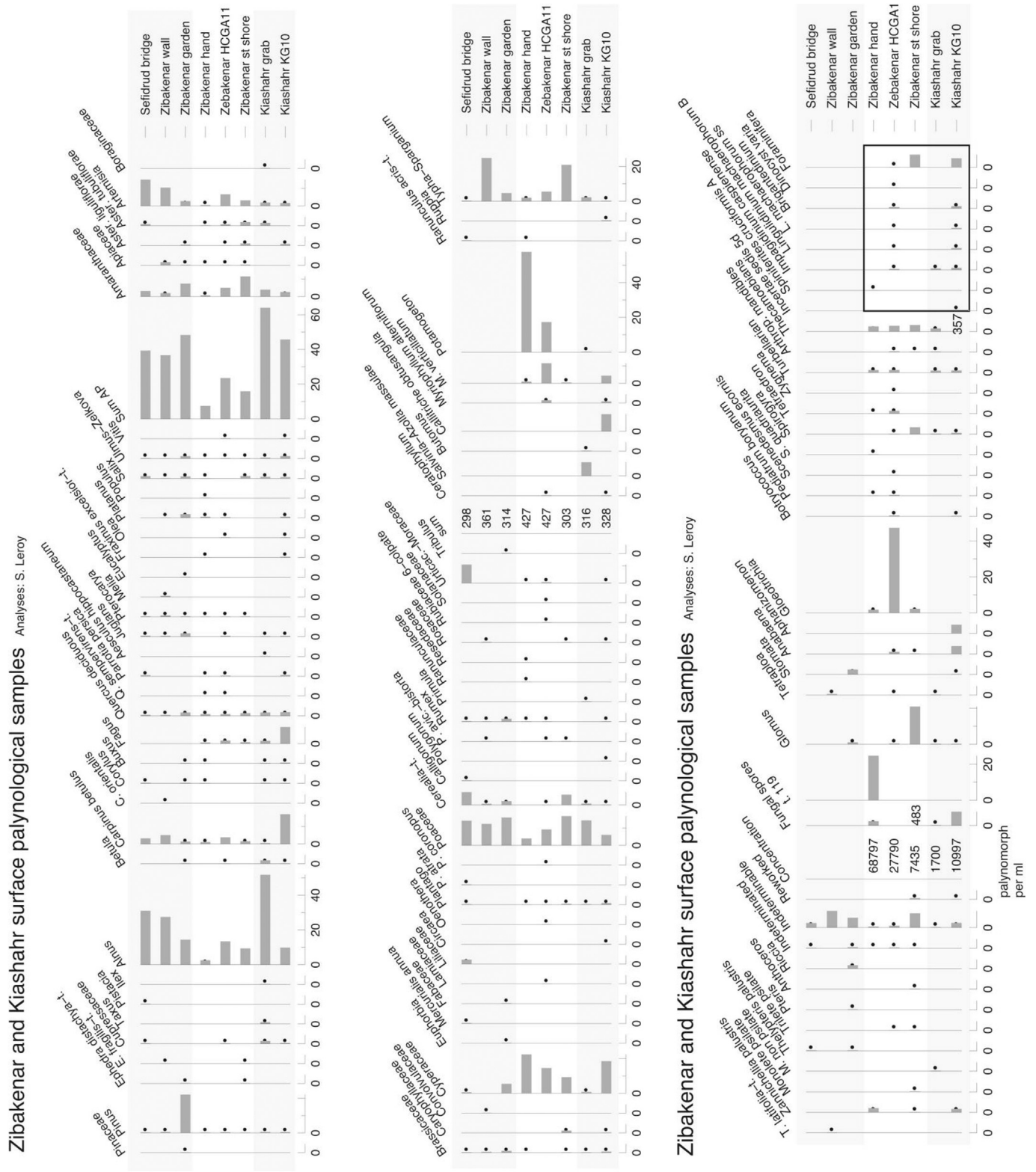

Fig. 12. Pollen, spores, non-pollen palynomorphs and dinocyst diagram for the surface samples. Black dot for values <0.5%.

Vitis. The NAP are dominated by Poaceae (18%) and *Artemisia* (11%). The Amaranthaceae values (5%) are the lowest of the diagram. *Salvinia–Azolla* massulae and microspores occur nearly exclusively in this zone. Dinocysts and foraminifer linings are frequent. Fungal spores are abundant.

Pz2, from 189 to 138 cm

A sharp decrease of *Alnus* occurs across this zone. Within this zone, *Pterocarya* becomes replaced by *Salix* that occupies a similar ecological niche. The occurrence of high values of *Vitis* and *Carpinus*

Fig. 13. Pollen, spores, non-pollen palynomorphs and dinocyst diagram. 10× exaggeration curve. Black dot for values <0.5%. Rectangle around the dinocysts and foraminifera.

ends at the top of this zone. On the contrary, the start of the development of *Platanus*, *Olea*, *Juglans* and *Parrotia persica* is observed at the base of this zone. In the NAP, Amaranthaceae and Asteraceae displayed a progressive increase. Poaceae values remained constant around 9%. The values of dinocysts and foraminifers drop from the base of this zone to its top. Fungal spores reach a minimum, still 50–90% of the pollen sum, in the middle of this zone.

Pz3, from 138 cm to top

Alnus displays the lowest values in this zone, i.e. only 3–21%. A grain of *Eucalyptus* pollen is found at 66.5 cm depth. The other tree pollen do not increase; hence the AP% is the lowest (16–43%). In the NAP, Amaranthaceae and *Artemisia* reached at first a maximum of 30 and 20%, respectively, then decrease slowly. The continuous presence of Poaceae, Cyperaceae and Plantaginaceae is recorded. It is noteworthy to indicate that the lowest three samples of this zone, between 134 and 86 cm depth, are devoid of freshwater algae remains and of dinocysts. This depth range also contained three barren samples (114–94 cm; grey strip on Fig. 13) and the maxima of fungal spores (i.e. 261% of the pollen sum). From 66 cm depth upwards, the presence of algal spores and of some dinocysts and foraminifers is again noted. Fungal spores and *Glomus* are generally extremely abundant. The uppermost sample (0.5 cm) contained a single peak of *Myriophyllum spicatum* and of *Gloeotrichia*, as well as a drop in the fungal spore values.

4.5. Chronology

^{210}Pb activity measured on the top section of ZL11L2A1 appeared to reach equilibrium with the supported ^{210}Pb activity at a depth of about 74 cm (at the base of the top section). However, total ^{210}Pb and supported ^{210}Pb activities in the lower sediments (Fig. 14 A) suggest that the apparent equilibrium depth at c. 74 cm might have been due to dilution by fast sediment accumulation. Moreover, unsupported ^{210}Pb activities, calculated by subtracting supported ^{210}Pb activity from total ^{210}Pb activity, vary very irregularly with depth, and show little net decline between 2 and 72 cm (Fig. 14 B), suggesting an increasing upward trend in sediment accumulation.

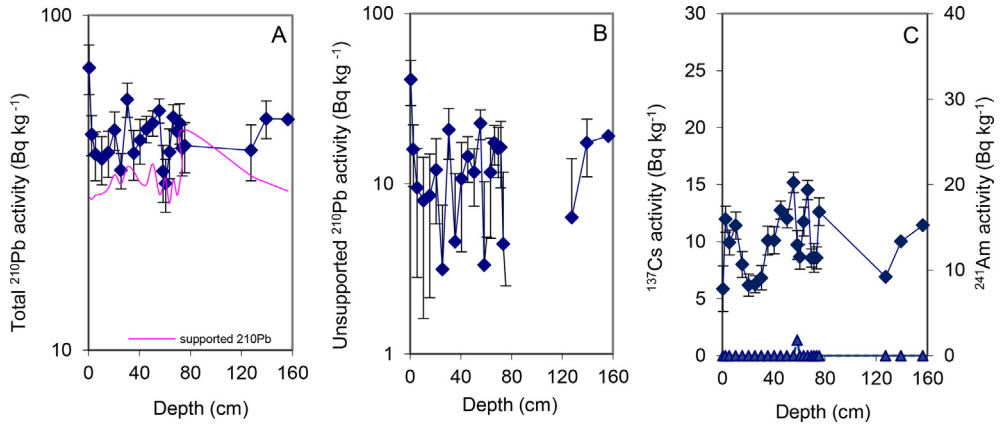

Fig. 14. Fallout radionuclide concentrations in core ZL11L2A taken from Zibakenar Lagoon, showing A: total ^{210}Pb, B: unsupported ^{210}Pb, and C: ^{137}Cs (diamond at the top) and ^{241}Am (triangle at the bottom) concentrations versus depth.

The ^{137}Cs activity versus depth profile has poorly resolved peaks between 35 and 67 cm. Detectable ^{241}Am at 58–59 cm (Fig. 14C) suggests fallout from the atmospheric testing of nuclear weapons that peaked in 1963. Similar to the unsupported ^{210}Pb activities between 58 and 61 cm, the relatively low level of ^{137}Cs activities in the same section is likely to be a result of sediment dilution. High sediment accumulation may have occurred at the time when maximum deposition has removed the ^{137}Cs peak away from 56 to 63 cm. Deeper samples also showed ^{137}Cs concentrations, suggesting a post-1950 date. However, no further detection of ^{241}Am was possible in these levels. In the light of the results of both ^{210}Pb and ^{137}Cs, radionuclide chronologies can only provide a suggested chronology for post-1950 above 156 cm depth due to high and irregular accumulation rates in this sequence.

From the third core section, three radiocarbon dates were obtained from two pieces of wood and one shell (*C. glaucum*) at depths of 209 (Sz2), 177 (Sz3) and 171 cm (Sz2), respectively (Table 3 and Fig. 8). Radiocarbon dating places AD 30 at 209 cm, which is very different from the other dating results and has been rejected due to the possibility of reworking. Other indicators of sediment reworking in sequence Sz1 are discussed below. Samples located at 177 and 171 cm exhibited post-bomb radiocarbon activities. CALIBomb is inappropriate for calibrating marine samples, such as the shell sample at 171 cm, as the ocean's uptake of bomb carbon was much slower and less dramatic than that of the atmosphere. At the moment no agreed calibration curve exists for the oceans (R. Reimer, pers. comm.). Therefore, only the sample at 177 cm could be used in our interpretation.

Spheroidal carbonaceous fly-ash particles (SCPs) are present in low but detectable concentrations in ZL11L2A1 above 65 cm depth. Below 65 cm, no SCPs are observed. In lakes with high sediment accumulation rates, the start of the SCP record often occurs in c. 1950, when an increase in contamination from high temperature fossil-fuel combustion increases SCP inputs from below to above the analytical limit of detection for the first time. This is seen at many sites across the world (Rose, 2015), and would suggest that in ZL11L2A1, 65 cm could be ascribed a 1950 date in agreement with the tentative radiometric chronology. SCP data cannot provide additional evidence for a recent date for the lower section of the core, but their absence could simply be due to a combination of low concentrations and high sediment accumulation rate diluting the signal.

5. Discussion

5.1. The development of the coastal lagoons

Based on aerial photograph from 1955 (Fig. 3A), the Sefidrud Delta prograded into the CS with a north-east trend. High sediment supply resulted in an eagle head shaped delta and even the formation of islands in the Sefidrud mouth. The sand barrier that in a later stage determined the formation of the Kiashahr Lagoon had already started to form.

Between 1955 and 1964 (Fig. 3A and B), a minor avulsion occurred and the Sefidrud direction changed westwards. Further sand barriers were formed and as a result two lagoons came into existence on the west side of the Sefidrud: Zibakenar and Ushmak. The latter was formed at the mouth of the Ushmak River. This small avulsion from east to west had a strong impact on the formation of Ushmak and Zibakenar Lagoons by providing more sediment to the western half of the delta, which resulted in the formation of the sand spits.

During the years from 1964 to 1982 (Fig. 3B and C), Zibakenar and Ushmak Lagoons developed further. The natural inlet from the CS to the enclosing Kiashahr lagoon became narrower and migrated to the south as the spit grew. The Sefidrud direction changed from

Table 3
Radiocarbon dates from Queen's University Belfast, calibrated ages are reported for 2σ range with highest probabilities shown in parentheses.

Laboratory number	Sample ID	Depth (cm)	Material type	^{14}C Age (yr BP)	F^{14}C	Calibration programme	Calibrated (2σ range)	Median probability
UBA- 22722	ZL2A3-7	171	Shell (*C. glaucum*)	modern	1.1174 ± 0.0031	–	–	*
UBA-25613	ZL11L2A3-12-14 cm	177	Wood (root)	modern	1.0326 ± 0.0056	CALIBomb with NHZ2	AD 1955–1956 (95.4%)	*
UBA-23787	ZL11L2A3-44-46 cm	209	Wood (branch)	1971 ± 31	0.7824 ± 0.0030	CALIB 7.1 with Intcal13	BC 45- AD 85 (95.4%)	AD 30

*Median probabilities on the CALIBomb programme output are not available, because the ages obtained from CALIBomb are not sufficiently widely spaced (P. Reimer, pers. comm.).

north-west to north and the active channel belt became narrower. This reflects the impact of reducing Sefidrud sediment supply as a result of the construction of the Manjil Dam in 1962 (Table 1). Despite this, the delta progradation remained constant due to continuous sea level fall that ended only in 1977 (Fig. 1).

From 1977 until 1995, sea level in the CS rose rapidly (Fig. 1). During the years from 1982 to 1991 (Fig. 3C and D), the Sefidrud Delta progradation rate was higher than in the previous period, as a result of the Manjil Dam flushing operations from the early 1980s, with a peak in 1984–1985 (Table 1), which resulted in an arrow-like shaped delta. Therefore, despite continuous sea level rise from 1977 to 1995, the delta continued to prograde. At the same time, erosion in the Kura delta in nearby Azerbaijan (Fig. 2A) increased and coastlines retreated 10–15 m (Kaplin and Selivanov, 1995). In 1991, a minor tributary of the Sefidrud started to form in the east, between Kiashahr lagoon and the main tributary of the Sefidrud (Fig. 3D).

Between 1991 and 2014 (Fig. 3D and E), a minor river avulsion happened and the Sefidrud changed its course from N to NE. The minor tributary of the Sefidrud (Fig. 3D) became the main tributary in 2014. Erosion increased in the western part of the Sefidrud Delta. By 2014, the navigable connection with the CS had ceased to exist and the Zibakenar Lagoon became choked and completely isolated (Fig. 3E). If a 'natural' evolution had continued, the water body would have become progressively infilled by land-derived sediments, introduced mainly by the Sefidrud. At the same time, a rapid infill by sediment and *Phragmites* and *Typha australis* plants occurred in the Kiashahr Lagoon (Fig. 3E; Naqinezhad, 2012; Ramsar Report 37, 2015).

5.2. Age validation and sedimentation rates in Zibakenar Lagoon

A multiple dating approach including radionuclide dating and radiocarbon dating, indirect biotic dating (based on known arrival dates for immigrant plant and bivalve species) and evidence from SCPs and remote sensing was applied on core ZL11L2 and Zibakenar Lagoon. The radionuclide chronology shows that sediments shallower than 156 cm are more recent than 1950. Radiocarbon age estimates were 1955–1956 at 177 cm (Fig. 15). These data are corroborated by biological time–marker elements. One pollen grain of *Eucalyptus* (a tree introduced from the southern hemisphere) was found at 66.5 cm depth. *Eucalyptus* trees were introduced not earlier than 1952 in the Hyrcanian forests, and only became abundant after 1970 (Sagheb–Talabi, 2004; Akhani et al., 2010). The other time marker that can be used to validate the dating is the occurrence of the invasive bivalve *A. segmentum*. This bivalve was brought from the Azov–Black Sea into the Caspian in 1939–1940 and by the end of 1959 it populated the western part of the middle and southern CS (Grigorovich et al., 2003). The presence of juvenile *A. segmentum* at 217 cm depth confirms that the whole sequence was probably formed after 1959. Only larval shells of *A. segmentum* were found, which eliminate any concern about burrowing. Remote sensing also confirms that the Zibakenar Lagoon was formed between 1955 and 1964 (Fig. 3A and B).

To sum up, these time markers, together with remote sensing results, are in agreement with the results of radiocarbon dating (1955 at 177 cm), which provides an approximate sedimentation rate of 3.1 cm y^{-1}. Therefore, this lagoon is younger than what has been suggested by previous research in the area (i.e. 'last four centuries' in Lahijani et al., 2009 and 'after 1880' in Naderi Beni et al., 2013b), and older than what has been suggested by Kazancı and Gulbabazadeh (2013), i.e. 1982. Other lagoons in the southern CS, including Anzali, Amirkola, and Gorgan Bay have shown relatively low sedimentation rates (Table 4).

Table 4
Sedimentation rates in lagoons of the southern Caspian Sea.

Site name	Sedimentation rate (cm yr^{-1})	References
Gorgan Bay	0.5	Amini et al. (2012)
Anzali	0.1–0.6	Leroy et al. (2011)
Amirkola	0.25	Leroy et al. (2011)
Karabogaz Gol	0.46	Leroy et al. (2006)

5.3. 20th Century depositional sedimentary environments of Zibakenar lagoon

Different zonations based on sedimentology, macro–remains and palynology proxies (Sz, Mz and Pz) are combined and presented in Fig. 15. The proxy zonations are in close agreement. Small discrepancies are mostly due to differences in sampling resolution. The combination of the different proxies allows to recognition of four main depositional environments, from bottom to top:

I: Estuary phase (220–182 cm)

Estuarine facies are found in the deepest part of the sequence ZL11L2 (A and B), ZL11L1 (A and C), ZL11G2 and ZL11G7 and has high MS values, indicating a terrestrial source for the sediments. Nevertheless, it is also characterised by the presence of typical Caspian fauna including bivalves such as *A. segmentum*, *C. glaucum*/*M. edentula* and foraminifers such as *A. beccarii*, a typical inhabitant of silty–sandy grounds of the CS (Latypov, 2004). Dinocysts and foraminifers are abundant. Hence, CS and fluvial sediment sources contributed to the formation of this facies. The presence of charophytic oogonia, the reproductive body of a multicellular green algae encrusted by limestone, does not contradict the interpretation of a marginal marine environment. Charophytes tolerate a wide range of salinities, from fresh to hypersaline, though they do not occur in normal marine environments due to the high energy (García et al., 2002).

The plant material encountered may have been transported by river, possibly explaining the 'old' radiocarbon age on a wood sample at 209 cm depth. Also, high concentrations of *Alnus* pollen were found in this unit; the site is probably not in the alder swamp itself, but under its strong influence as the trees would have vanished if they were under the direct influence of saline waters. In brief, this environment may correspond to an estuary of a minor distributary of the Sefidrud.

II: Open lagoon phase (182–147 cm)

Deposition of lagoonal sediment containing both charophytes and typical CS bivalves (such as *A. segmentum* and *M. edentula*/*C. glaucum*), and foraminifers (*A. beccarii*) is indicative of the beginning of the separation from the open CS through formation of a sand barrier. This facies is found in cores ZL11L2 (A and B), ZL11L1 (A, B and C). A clear change in sediment colour at the top of this facies (at 151 cm depth) suggests a transitional zone between the open lagoon to the successive closed lagoon. This transitional zone contains a small amount of dinocysts, but foraminifers are absent. The alder swamp is nearby in phase I, but its progressive disappearance occurs in phase II. Based on the results of radiocarbon dating, the formation of a coastal lagoon under brackish water invasion can be dated to

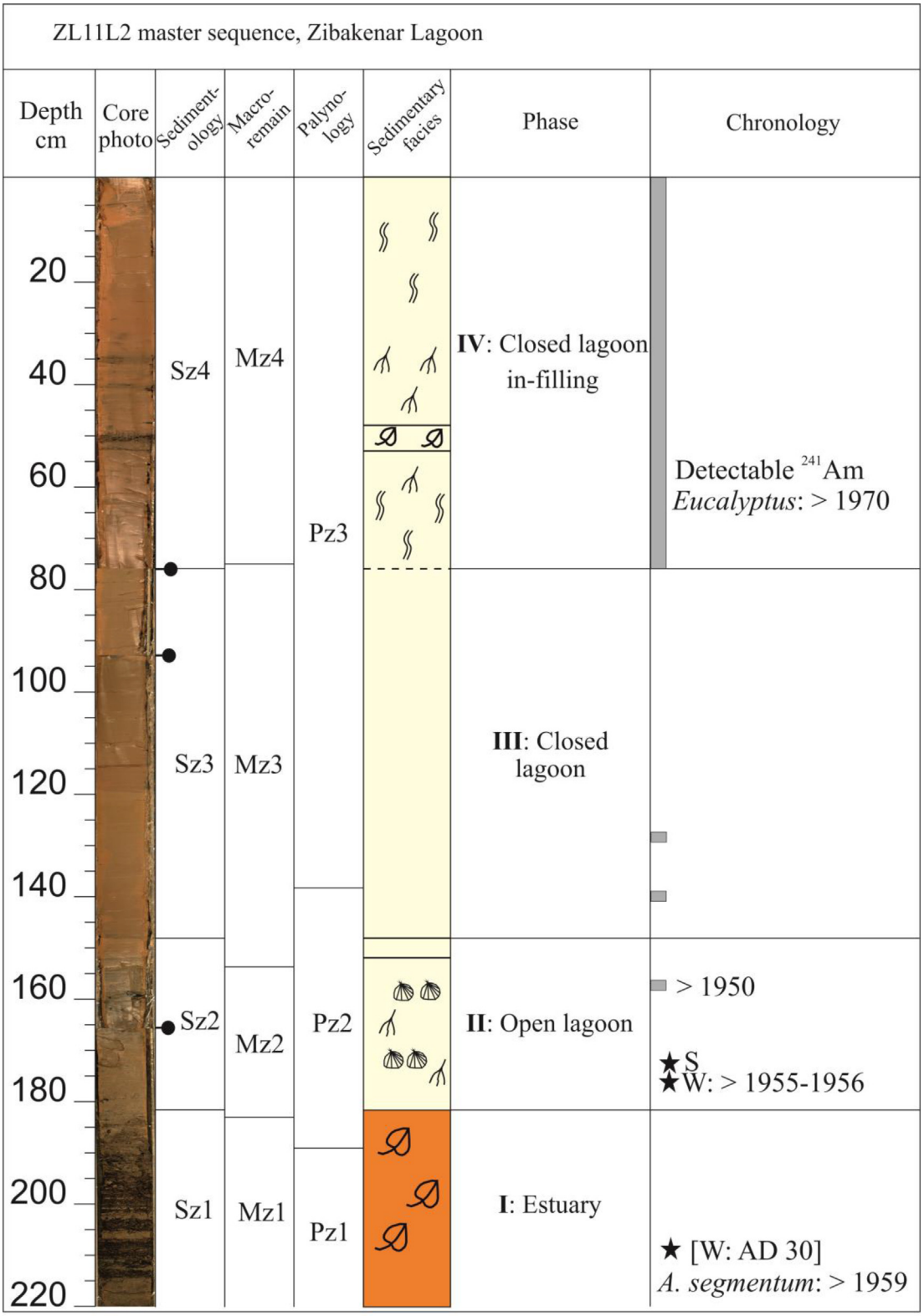

Fig. 15. Comparison of different zones, including sedimentology (Sz), macro-remains (Mz) and palynology (Pz), and depositional environments in ZL11L2A master sequence. Grey strip and rectangles: radionuclide dating. Black stars: ^{14}C, W: wood and S: shell (material dated). The radiocarbon age of AD 30 at 209 cm is rejected. (For legend of sedimentary facies see Fig. 7).

1955–1956. However, as *A. segmentum* was already found in the preceding phase, this environment dates from after 1959.

III: Closed lagoon phase (147–76 cm)

The replacement of typical CS molluscs by fossil–poor, fine–-grained deposits reflects a decrease in brackish water influence and the build–up of a continuous sand barrier protecting the lagoon from the sea. Part of this silty sequence is even devoid of palynomorphs and has an orange shine from 118 to 90 cm depth, probably caused by oxidation and/or strong soil influx. As the two surface samples from the Sefidrud were devoid of pollen, it is not unlikely that the river was the source for lagoonal deposits. Therefore, sediment may have been transported through flushing operations at Manjil Dam since 1980 and most likely in the peak years 1984 and 1985 (Table 1). This would have instantaneously transported large amounts of fine–grained sediment downstream, killing fish and modifying phytoplankton communities (Morris and Fan, 1998; Pourafrasyabi and Ramezanpour, 2014). In this environment (environment III) and also the final phase (IV), pollen grains of Alder can be used as a taphonomical indicator of long–-distance transport. Pollen analysis suggests the occurrence of rice paddies and wetlands in the drainage.

IV: Closed lagoon in-filling phase (76–0 cm)

The fourth and last phase corresponds to terrestrial deposition that includes fine sediments. A brief brackish water incursion is indicated by considerable amounts of foraminifers (*A. beccarii*), dinocysts and also broken bivalve shells at a depth of 66 cm, which could be related to maximum sea level rise at 1995. The increased abundance of aquatic vegetation spores and pollen and decrease of fungal spores and *Glomus* in the top sample may represent re–vegetation as a result of increased protection offered by the Nature Park status acquired in 2001.

5.4. Evolution of the Zibakenar lagoon through time and related sea levels

Based on the four phases and key layers such as sterile and transitional zones in the third phase, discussed in the previous section, the cores were correlated and an internal sediment distribution pattern in the Zibakenar Lagoon obtained (Fig. 16).

The Zibakenar infill has the typical form of a lagoon (Bungenstock and Schäfer, 2009; Costas et al., 2009) in which the fine sediment accumulation is larger in its centre (e.g. cores ZL11L1 (A and B) and ZL11L2 (A–C)), sandy at the bottom (e.g. cores ZL11L1, ZL11L2 and ZL11G7) and organic rich at the margins (gravity cores ZL11G1, ZL11G3, ZL11G4 and ZL11G6). Oertel et al. (1992) showed that lagoons that have developed along tide–dominated coasts typically have floors that are irregular, reflecting the antecedent bottom topography. By contrast, lagoons developed along wave–-dominated coasts tend to have a simple floor–topography.

Fine sediment thicknesses reach up to 182 cm. The boundary between phases I and II (Fig. 16) represent the time of lagoon formation. The ZL11L2 sequence illustrates the progressive decline of the alder swamp and the opening of the landscape in a strongly erosive catchment, with a peak of eroded product input at 134 to 86 cm, likely due to dam flushing operation peak in 1984–1985 (Table 1). The decline of the CS influence is due to the delta progradation and minor changes in the Sefidrud distributary.

The evolution of Zibakenar Lagoon can be divided into three stages based on whether the area was transgressive, regressive, or almost stationary relative to sea–level. The lagoon originated between 1955 and 1964 as a result of Sefidrud Delta progradation into the CS in a period when sea level was relatively stable. During that period, long–shore currents formed a sand spit and Zibakenar Lagoon came into existence. The lagoon had inlets to the CS as shown by the presence of CS bivalves, foraminifers and dinocysts. In the next stage, the coastal embayment became enclosed by wave–built barriers. Along this wave-dominated stretch of coastline, the wave induced long-shore sediment transport resulted in formation and growth of a spit. The same process can lead to a progressive choking of the lagoon, decreasing its equilibrium volume (Duck and da Silva, 2012). The response to sea-level fluctuation of a lagoon is a function of sedimentation rate and sea level rise (Nichols and Boon, 1994; Kirk and Lauder, 2000). An increasing sedimentation rate, while the rate of sea level rise is low, yields a surplus lagoon where the lagoon is infilling and short-lived. In contrast, when sea level rise exceeds sedimentation rate, the lagoon gains volume (Nichols and Boon, 1994; Kirk and Lauder, 2000). Between 1977 and 1995, sea level rose and Zibakenar was

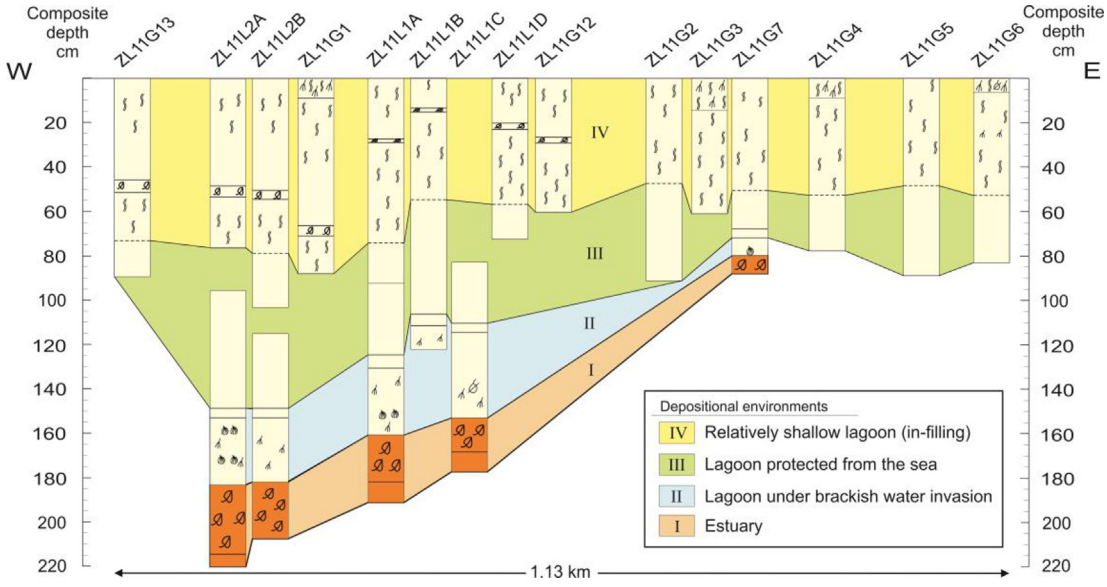

Fig. 16. Correlation of cores in Zibakenar Lagoon based on four sedimentary facies (For legend of sequences see Fig. 6.).

flooded by the CS. The maximum CS level rise of 1995 is recognisable by the presence of CS indicators (Fig. 11 and 13). The connection of Zibakenar Lagoon with the CS is also visible in remote sensing data (Fig. 3D). Since 1995, the CS has been falling and sediment supply from the Sefirud restricted due to the lack of flushing operations since 1998 (Table 1; Yamani et al., 2013).

5.5. Future of the coastal lagoons

The most common scenario of lagoon evolution is the so-called diverging model (Oertel et al., 1992), which describes coastal lagoonal evolution as being driven by sediment infill and therefore coastal lagoons have been considered to be natural sediment sinks (Boyd et al., 1992; Nichols and Boon, 1994). The Zibakenar, Ushmak and Kiashahr lagoons are located in the active growing Sefidrud Delta with high sedimentation rates and can be categorised as surplus lagoons. The present study demonstrated their very recent appearance between 1955 and 1964. It can also be reasonably predicted that the lagoons will be filled relatively soon because of the high sedimentation rates in the Zibakenar Lagoon (c. 3.1 cm/y). If this rate is used, the middle of the lagoon, that is now under 185 cm of water, will be filled in 59 years. The total longevity of the Zibakenar Lagoon would then only be c. 115 years. Such a short duration is not unusual for coastal lagoons (Oertel et al., 1992; Martin and Dominguez, 1994; Kirk and Lauder, 2000; Duck and da Silva, 2012).

The CS is a special case as sea level rises and falls are much faster than the global ocean and hence lagoons may appear and disappear much faster (Ignatov et al., 1993; Kaplin et al., 2010). This provides additional constraints on conservation of lagoons around the CS not seen in marine coastlines elsewhere. The CS has a coastline of the order of 7000 km long, which is punctuated by many lagoons (Ignatov et al., 1993). Many have known similar history to that of Zibakenar, for example the Caspijsk Lagoon in Dagestan. Conservation often is aiming at preserving steady-stable environments while the Sefidrud Delta and its lagoons are extremely dynamic. Future plans by the Ramsar Convention for the adequate protection of the Boujagh National Park (and many other lagoons around the CS) should take the dynamic behaviour of the lagoons into consideration if they want to maintain its high biodiversity and shelter role for regionally rare species and migrating birds. The condensed evolution history of the CS lagoons should be considered when evaluating changes happening to coastlines around the world threatened by flooding due to the current sea level rise.

6. Conclusions

Remote sensing and sedimentology and palynology analyses on Zibakenar Lagoon show that this lagoon alongside the Boujagh lagoons in the Sefidrud Delta developed from an embayment separated from the CS by a sand spit, when the sea level was stable. Therefore, development of these lagoons was not a response to sea level rise. Along the wave-dominated CS coastline, the wave induced long–shore sediment transport promoted the formation and growth of a sand spit that, through time, progressively enclosed the inlet. Subsequently, rapid sea-level rise between the years 1977 and 1995 and Manjil Dam flushing from 1980 to 1998 provoked a rapid sedimentation in the lagoons. These short-lived shallow lagoons may fill up even more rapidly if the Sefidrud is diverted into them by future avulsion events. The evolution of these lagoons will depend on the relative interactions of CS level change, sediment supply, river avulsion and human activity. The situation in the CS is quite unique in the very dynamic character of the various processes that drive lagoonal evolution and consequently make conservation of Caspian lagoons challenging. This dynamic character makes the Caspian Sea a natural laboratory for sea level rise and climate change studies relevant at a global level. As a final point, revision by the Ramsar Convention Secretariat is required to incorporate the need to remain flexible, as lagoons may appear and disappear relatively fast. This would be essential to maintain the future quality of a Ramsar site on the south coast of the Caspian Sea.

Acknowledgements

This research is part of the PhD of the first author entitled “Evaluation of Sefidrud Delta (South West Caspian Sea) during the last millennium”, which was funded by Brunel University London (Grant No.: R85104). The publication is a contribution to the INQUA QuickLakeH project (No 1227) and to the European project Marie Curie, CLIMSEAS–PIRSES–GA–2009–247512. Iranian National Institute for Oceanography and Atmospheric Science (INIOAS) is especially thanked for organising field campaign. We would also like to acknowledge Dr Handong Yang (University College London) for his contribution in radionuclide dating and Mr Naser Ghasemi (INIOAS) for his assistance in the field.

Appendix A

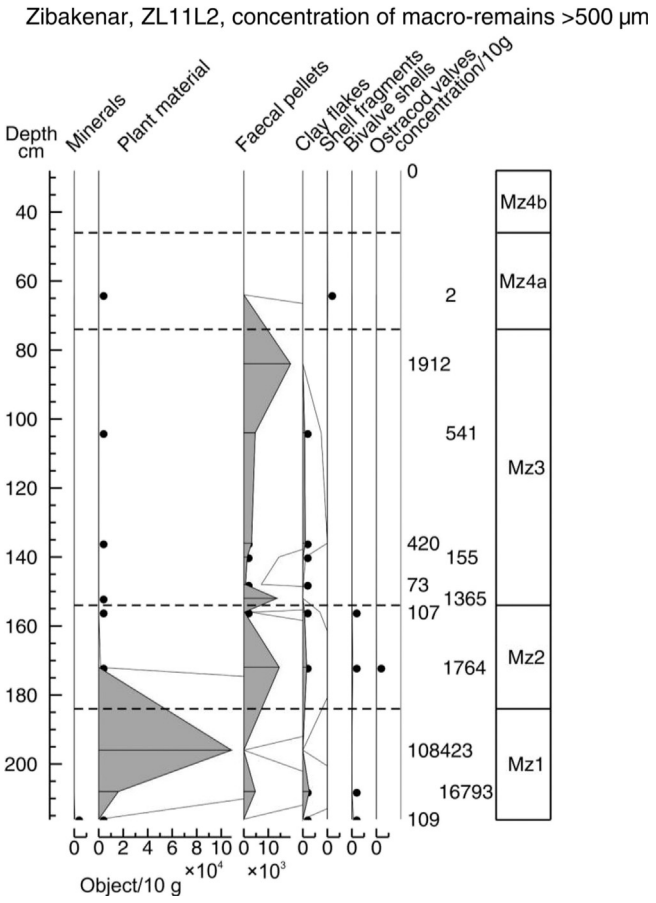

Fig. A1. The concentration of macro-remains >500 µm in the master sequence ZL11L2. The black dots represent very low concentrations of macro-remains.

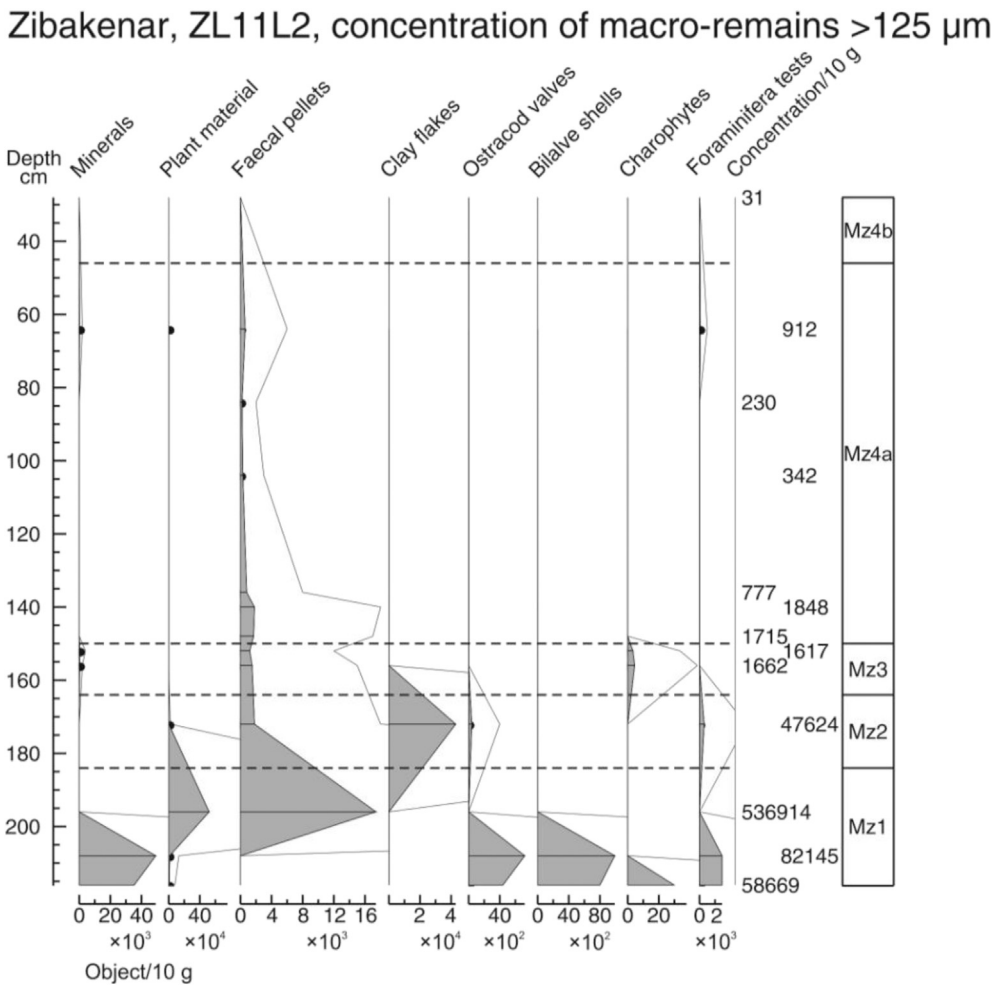

Fig. A2. The concentration of macro-remains >125 μm in the master sequence ZL11L2. The black dots represent very low concentrations of macro-remains.

References

Akhani, H., Djamali, M., Ghorbanalizadeh, A., Ramezani, E., 2010. Plant biodiversity of Hyrcanian relict forests, N Iran: an overview of the flora, vegetation, palaeoecology and conservation. Pakistan Journal of Botany 42, 231–258.

Amini, A., Mousavi Harami, R., Lahijani, H., Mahboubi, A., 2012. Holocene sedimentation rate in Gorgan Bay and adjacent coasts in southeast of Caspian Sea. Journal of Basic and Applied Scientific Research 2 (1), 289–297.

Annotated Ramsar List, 2011. http://ramsar.rgis.ch/cda/en/ramsar-documents-list-anno-iran/main/ramsar/1-31-218%5E16557_4000_0__ (last accessed 13.03.15.).

Appleby, P.G., Richardson, N., Nolan, P.J., 1992. Self–absorption corrections for well–type germanium detectors. Nuclear Instruments and Methods B 71, 228–233.

Appleby, P.G., Nolan, P.J., Gifford, D.W., Godfrey, M.J., Oldfield, F., Anderson, N.J., Battarbee, R.W., 1986. ^{210}Pb dating by low background gamma counting. Hydrobiologia 141, 21–27.

Arpe, K., Leroy, S.A.G., Lahijani, H., Khan, V., 2012. Impact of the European Russia drought in 2010 on the Caspian Sea level. Hydrology and Earth System Sciences 16 (1), 19–27.

Aslan, A., Autin, W.J., 1999. Evolution of the Holocene Mississippi River floodplain, Ferriday, Louisiana: insights on the origin of fine–grained floodplains. Journal of Sedimentary Research 69 (4), 800–815.

Aslan, A., Autin, W.J., Blum, M.D., 2005. Causes of river avulsion: insights from the late Holocene avulsion history of the Mississippi River, USA. Journal of Sedimentary Research 75 (4), 650–664.

Bennett, K., 2007. Psimpoll and Pscomb Programs for Plotting and Analysis. Version 4.27. www.chrono.qub.ac.uk/psimpoll/psimpoll.html (last accessed 16.01.15.).

Blott, S.J., Pye, K., 2001. GRADISTAT: a grain size distribution and statistics package for the analysis of unconsolidated sediments. Earth Surface Processes and Landforms 26 (11), 1237–1248.

Birks, H.H., 2001. Plant macrofossils. In: Smol, J.P., Birks, H.J.B., Last, W.M. (Eds.), Tracking Environmental Change Using Lake Sediments. Springer, pp. 49–74.

Boyd, R., Dalrymple, R., Zaitlin, B., 1992. Classification of clastic coastal depositional environments. Sedimentary Geology 80 (3), 139–150.

Bungenstock, F., Schäfer, A., 2009. The Holocene relative sea–level curve for the tidal basin of the barrier island Langeoog, German Bight, Southern North Sea. Global and Planetary Change 66 (1), 34–51.

Costas, S., Sobrino, C.M., Alejo, I., Pérez–Arlucea, M., 2009. Holocene evolution of a rock–bounded barrier lagoon system, Cíes Islands, northwest Iberia. Earth Surface Processes and Landforms 34 (11), 1575–1586.

Dolotov, Y., Kaplin, P., 2005. Black and Caspian Seas, coastal ecology and geomorphology. In: Encyclopedia of Coastal Science. Springer, pp. 194–203.

Doriniana, T.A., Myakokin, V.S., 1972. Sediment transport along the western Caspian Coast, according to their mineralogical analysis. Comprehensive Study of the Caspian Sea 3, 147–154 (in Russian).

Duck, R.W., da Silva, J.F., 2012. Coastal lagoons and their evolution: a hydromorphological perspective. Estuarine, Coastal and Shelf Science 110, 2–14.

Farley Nicholls, J., Toumi, R., 2014. On the lake effects of the Caspian Sea. Quarterly Journal of the Royal Meteorological Society 140 (681), 1399–1408.

Folk, R.L., 1974. Petrology of Sedimentary Rocks (Hemphill, Texas).

García, A., Jones, B.G., Chenhalland, B.E., Murray–Wallace, C.V., 2002. The charophyte *Lamprothamnium succinctum* as an environmental indicator: a Holocene example from Tom Thumbs Lagoon, eastern Australia. Alcheringa 26 (4), 507–518.

Grigorovich, I.A., Therriault, T.W., MacIsaac, H.J., 2003. History of aquatic invertebrate invasions in the Caspian Sea. Biological Invasions 5, 103–115.

Heiri, O., Lotter, A.F., Lemcke, G., 2001. Loss on ignition as a method for estimating organic and carbonate content in sediments: reproducibility and comparability of results. Journal of Paleolimnology 25 (1), 101–110.

Heyvaert, V.M.A., Baeteman, C., 2008. A Middle to Late Holocene avulsion history of the Euphrates river: a case study from Tell ed–Dēr, Iraq, Lower Mesopotamia. Quaternary Science Reviews 27 (25), 2401–2410.

Hoogendoorn, R.M., Boels, J.F., Kroonenberg, S.B., Simmons, M.D., Aliyeva, E., Babazadeh, A.D., Huseynov, D., 2005. Development of the Kura delta, Azerbaijan; a record of Holocene Caspian sea–level changes. Marine Geology 222, 359–380.

Hua, Q., Barbetti, M., Rakowski, A.Z., 2013. Atmospheric radiocarbon for the period 1950–2010. Radiocarbon 55 (4), 2059–2072.

Ignatov, Y.I., Kaplin, P.A., Lukyanova, S.A., Solovieva, G.D., 1993. Evolution of the Caspian Sea coasts under conditions of sea-level rise: model for coastal change under increasing "greenhouse effect". Journal of Coastal Research 104–111.
Jones, L.S., Schumm, S.A., 2009. Causes of avulsion: an overview. In: Smith, N.D., Rogers, J. (Eds.), Fluvial Sedimentology VI. Blackwell Publishing Ltd, Oxford, UK, pp. 171–178.
Kaplin, P., Selivanov, A., Lukyanova, S., 2010. Azerbaijan. In: Bird, E. (Ed.), Encyclopedia of the World's Coastal Landforms. Springer Science & Business Media, pp. 885–888.
Kaplin, P.A., Selivanov, A.O., 1995. Recent coastal evolution of the Caspian Sea as a natural model for coastal responses to the possible acceleration of global sea–level rise. Marine Geology 124 (1), 161–175.
Kazancı, N., Gulbabazadeh, T., 2013. Sefidrud delta and quaternary evolution of the southern Caspian Lowland, Iran. Marine and Petroleum Geology 44, 120–139.
Kazancı, N., Gulbabazadeh, T., Leroy, S.A.G., Ileri, O., 2004. Sedimentary and environmental characteristics of the Gilan-Mazenderan plain, northern Iran: influence of long- and short-term Caspian water level fluctuations on geomorphology. Journal of Marine Systems 46, 145–168.
Khoshraftar, R., 2005. Geomorphological evolution Kiashahr lagoon using aerial photographs and satellite images and GPS. In: Proceedings of the 9th International Conference on Environmental Science and Technology. Rhodes Island, Greece, pp. 381–387.
Khosronejad, A., 2009. Optimization of the Sefid–Roud Dam desiltation process using a sophisticated one–dimensional numerical model. International Journal of Sediment Research 24 (2), 189–200.
Kirk, R.M., Lauder, G., 2000. Significant Coastal Lagoon Systems in the South Island, New Zealand: Coastal Processes and Lagoon Mouth Closure. Science for Conservation 146. Department of Conservation, Wellington, New Zealand.
Kosarev, A.N., 2005. Physico–geographical conditions of the Caspian Sea. In: Kostianoy, A., Kosarev, A. (Eds.), The Caspian Sea Environment. Springer, pp. 5–31.
Kousari, S., 1986. Evolution of sefidrud Delta. Development in Geological Education 1, 31–41 (in Persian).
Krasnozhon, G.F., Lahijani, H., Voropayev, G.V., 1999. Evolution of the delta of the Sefidrud River, Iranian Caspian Sea coast, from space imagery. Mapping Science and Remote Sensing 36, 256–264.
Kroonenberg, S.B., Abdurakhmanov, G.M., Badyukova, E.N., Borg, K.V.D., Kalashnikov, A., Kasimov, N.S., Rychagov, G.I., Svitoch, A.A., Vonhof, H.B., Wesselingh, F.P., 2007. Solar–forced 2600 BP and little Ice Age highstands of the Caspian Sea. Quaternary International 173, 137–143.
Kroonenberg, S., Badyukova, E., Storms, J., Ignatov, E., Kasimov, N., 2000. A full sea–level cycle in 65years: barrier dynamics along Caspian shores. Sedimentary Geology 134 (3), 257–274.
Lahijani, H.A.K., Rahimpour–Bonab, H., Tavakoli, V., Hosseindoost, M., 2009. Evidence for late Holocene highstands in central Guilan–East Mazanderan, south Caspian coast, Iran. Quaternary International 197 (1), 55–71.
Lahijani, H.A.K., Tavakoli, V., Amini, A.H., 2008. South Caspian river mouth configuration under human impact and sea level fluctuations. Environmental Sciences 5, 65–86.
Lepeshevkov, I.N., Buynevich, D.V., Buynevich, N.A., Sedel'nikov, G.S., 1981. Perspectives of Use of Salt Resources of Kara-bogaz-gol. Academia Nauka, Moscow, p. 273 (in Russian).
Latypov, Y.Y., 2004. Succession in the *Abra ovata* community on soft grounds of a newly flooded area of the Caspian Sea. Russian Journal of Ecology 35 (4), 267–273.
Leroy, S., Lahijani, H., Reyss, J., Chalié, F., Haghani, S., Shah–Hosseini, M., Shahkarami, S., Tudryn, A., Arpe, K., Habibi, P., 2013. A two–step expansion of the dinocyst *Lingulodinium machaerophorum* in the Caspian Sea: the role of changing environment. Quaternary Science Reviews 77, 31–45.
Leroy, S.A.G., 2010. Palaeoenvironmental and palaeoclimatic changes in the Caspian Sea region since the Lateglacial from palynological analyses of marine sediment cores. Geography, Environment, Sustainability 2, 32–41. Faculty of Geography of Lomonosov Moscow State University and by the Institute of Geography of RAS. http://www.geogr.msu.ru/GESJournal/.
Leroy, S.A.G., Tavakoli, V., Habibi, P., Naderi Beni, M., Lahijani, H.A.K., Djamali, M., Naqinezhad, A., Moghadam, M.V., Arpe, K., Shah–Hosseini, M., Hosseindoust, M., Miller, C.S., 2011. Late Little Ice Age palaeoenvironmental records from the Anzali and Amirkola Lagoons (south Caspian Sea): vegetation and sea level changes. Palaeogeography, Palaeoclimatology, Palaeoecology 302 (3), 415–434.
Leroy, S.A.G., Warny, S., Lahijani, H.A.K., Piovano, E.L., Fanetti, D., Berger, A.R., 2010. The role of geosciences in the mitigation of natural disasters: five case studies. In: Beer, T. (Ed.), Geophysical Hazards. Springer, pp. 115–147.
Leroy, S., Marret, F., Giralt, S., Bulatov, S., 2006. Natural and anthropogenic rapid changes in the Kara–Bogaz Gol over the last two centuries reconstructed from palynological analyses and a comparison to instrumental records. Quaternary International 150 (1), 52–70.
Makaske, B., 2001. Anastomosing rivers: a review of their classification, origin and sedimentary products. Earth–Science Reviews 53 (3), 149–196.
Marret, F., Leroy, S.A.G., Chalié, F., Gasse, F., 2004. New organic–walled dinoflagellate cysts from recent sediments of Central Asian seas. Review of Palaeobotany and Palynology 129 (1), 1–20.
Martin, L., Dominguez, J.M.L., 1994. Geological History of Coastal Lagoons. In: Elsevier Oceanography Series 60, pp. 41–68.
Mazzullo, J.M., Meyer, A., Kidd, R., 1988. New sediment classification scheme for the Ocean Drilling Program. In: Mazzullo, J.M., Graham, A.G. (Eds.), Handbook for Shipboard Sedimentologists, pp. 45–67. ODP Technical Notes 8.
Morris, G.L., Fan, J., 1998. Reservoir Sedimentation Handbook: Design and Management of Dams, Reservoirs, and Watersheds for Sustainable Use. McGraw Hill Professional, New York.
Naderi Beni, A., Lahijani, H.A.K., Harami, R.M., Arpe, K., Leroy, S.A.G., Marriner, N., Berberian, M., Andrieu–Ponel, V., Djamali, M., Mahboubi, A., 2013a. Caspian Sea level changes during the last millennium: historical and geological evidences from the south Caspian Sea. Climate of the Past 9, 1645–1665.
Naderi Beni, A., Lahijani, H., Harami, R.M., Leroy, S.A.G., Shah–Hosseini, M., Kabiri, K., Tavakoli, V., 2013b. Development of spit–lagoon complexes in response to Little Ice Age rapid sea–level changes in the central Guilan coast, South Caspian Sea, Iran. Geomorphology 187, 11–26.
Naqinezhad, A., 2012. A physiognomic–ecological vegetation mapping of Boujagh National Park, the first marine–land National Park in Iran. Advances in Bioresearch 3, 37–42.
Naqinezhad, A., Saeidi, M.S., Noroozi, M., Faridi, M., 2006. Contribution of the vascular and bryophyte flora as well as habitat diversity of Boujagh National Park, N. Iran. Rostaniha 7, 83–105.
Nichols, M.M., Boon, J.D., 1994. Sediment Transport Processes in Coastal Lagoons. In: Elsevier Oceanography Series 60, pp. 157–219.
Oertel, G.F., Kraft, J.C., Kearney, M.S., Woo, H.J., 1992. A rational theory for barrier lagoon development. In: Fletcher, C.H., Wehmiller, J.F. (Eds.), Quaternary Coasts of the United States 48SEPM, pp. 77–87.
Overeem, I., Kroonenberg, S., Veldkamp, A., Groenesteijn, K., Rusakov, G., Svitoch, A., 2003. Small–scale stratigraphy in a large ramp delta: recent and Holocene sedimentation in the Volga delta, Caspian Sea. Sedimentary Geology 159 (3), 133–157.
Pourafrasyabi, M., Ramezanpour, Z., 2014. Phytoplankton as bio–indicator of water quality in Sefid Rud River, Iran (South of Caspian Sea). Caspian Journal of Environmental Sciences 12 (1), 31–40.
Ramsar Report 37, 2015. www.ramsar.org/sites/default/files/documents/library/ram37e_iran.pdf (last accessed 16.04.15.).
Reimer, P.J., Bard, E., Bayliss, A., Beck, J.W., Blackwell, P.G., Ramsey, C.B., Buck, C.E., Cheng, H., Edwards, R.L., Friedrich, M., Grootes, P.M., Guilderson, T.P., Haflidason, H., Hajdas, I., Hatté, C., Heaton, T.J., Hoffmann, D.L., Hogg, A.G., Hughen, K.A., Kaiser, K.A., Kromer, B., Manning, S.W., Niu, M., Reimer, R.W., Richards, D.A., Scott, E.M., Southon, J.R., Staff, R.A., Turney, C.S.M., Plicht, J.V.D., 2013. IntCal13 and Marine13 radiocarbon age calibration curves 0–50,000 years cal BP. Radiocarbon 55 (4), 1869–1887.
Reimer, P.J., Brown, T.A., Reimer, R.W., 2004. Discussion: reporting and calibration of post–bomb ^{14}C data. Radiocarbon 46 (3), 1299–1304.
Renberg, I., Wik, M., 1984. Dating recent lake sediments by soot particle counting. Verhandlungen des Internationalen Verein Limnologie 22, 712–718.
Renberg, I., Wik, M., 1985. Soot particle counting in recent lake sediments: an indirect dating method. Ecology Bulletin 37, 53–57.
Rose, N.L., 2015. Spheroidal carbonaceous fly ash particles provide a globally synchronous stratigraphic marker for the Anthropocene. Environmental Science & Technology 49 (7), 4155–4162.
Rose, N.L., 2008. Quality control in the analysis of lake sediments for spheroidal carbonaceous particles. Limnology and Oceanography: Methods 6, 172–179.
Rose, N., Flower, R., Appleby, P., 2003. Spheroidal carbonaceous particles (SCPs) as indicators of atmospherically deposited pollutants in North African wetlands of conservation importance. Atmospheric Environment 37 (12), 1655–1663.
Rose, N., Harlock, S., Appleby, P., Battarbee, R., 1995. Dating of recent lake sediments in the United Kingdom and Ireland using spheroidal carbonaceous particle (SCP) concentration profiles. The Holocene 5 (3), 328–335.
Rose, N.L., 1994. A note on further refinements to a procedure for the extraction of carbonaceous fly–ash particles from sediments. Journal of Paleolimnology 11, 201–204.
Rucevska, I., Herberlin, C., Rekacewicz, P., Skaalvik, J.F., Baker, E., Novikov, V., Radvany, J., Demartino, L., 2006. Vital Caspian Graphics: Challenges beyond Caviar. UNEP/GRID, Arendal.
Sagheb–Talebi, K., 2004. Rehabilitation of temperate forests in Iran (Chapter 26). In: Stanturf, J.A., Madsen, P. (Eds.), Restoration of Boreal and Temperate Forests. CRC Press, New York, pp. 397–407.
Stuiver, M., Reimer, P.J., 1993. Extended ^{14}C database and revised Calib 3.0 ^{14}C age calibration program. Radiocarbon 35, 215–230.
Törnqvist, T.E., Snijders, Els MA., Storms, J.E., van Dam, R.L., Wiemannt, M.C., 1996. A revised chronology for Mississippi River subdeltas. Science 273, 1693–1696.
Törnqvist, T.E., 1993. Holocene alternation of meandering and anastomosing fluvial systems in the Rhine–Meuse delta (central Netherlands) controlled by sea–level rise and subsoil erodibility. Journal of Sedimentary Petrology 63, 683–693.
USDA, 2015. www.pecad.fas.usda.gov/cropexplorer/global_reservoir (last accessed 10.02.15.).
Yamani, M., Moghimi, E., Motamed, A., Jafarbeglo, M., Lorestani, G., 2013. Fast shoreline changes in Sefidrud Delta using transects analyses method. Physical Geography Research Quarterly 84 (2), 1–20 (in Persian).
Yousefi, A., Bahmanpour, H., Mafi, A., 2012. Survey of microhabitats use by birds in national parks (case study: wetland Boujagh National Park, Southwest Caspian Sea, Iran). Annals of Biological Research 3 (6), 2938–2946.